Biomaterials Science

ROYAL SOCIETY OF CHEMISTRY

REVIEW

View Article Online
View Journal | View Issue

Cite this: *Biomater. Sci.*, 2023, **11**, 76

Research progress of stimuli-responsive ZnO-based nanomaterials in biomedical applications

Zhenzhen Weng,[a] Yingying Xu,[b] Jie Gao[c] and Xiaolei Wang *[a,c]

Zinc oxide nanoparticles (ZnO NPs), an attractive oxide semiconductor material, are widely used in the biomedical field due to their good biosafety and economy. The proposal of stimuli-responsive materials provides a new way for the further application of single ZnO-based nanomaterials that cannot meet the ever-changing requirements. In this review, the emerging advances in exogenous stimuli (light, ultrasound, mechanical force, *etc.*) and endogenous stimuli (pH, enzymes, *etc.*) responsive systems of ZnO-based nanomaterials in biomedical applications are highlighted. First, the basic characteristics, response mechanisms and construction principles of single-stimulus-responsive ZnO-based nanomaterials, as well as their recent advances in tissue repair, medical devices and theranostics are summarized. Subsequently, the design method of multi-stimuli-responsive ZnO-based biomaterials is discussed, and the application advantages of multi-functional responsive systems are explained by analyzing typical cases of biomedical applications of multi-responsive strategies. Finally, we discuss the prospects for the design and development of stimuli-responsive ZnO-based biomaterials for biomedical applications and point out their advantages as well as the places that need to be further improved. The current review may provide a useful reference for researchers interested in constructing such abundant, inexpensive and widely applicable multi-stimuli-responsive materials.

Received 8th September 2022,
Accepted 9th October 2022

DOI: 10.1039/d2bm01460b

rsc.li/biomaterials-science

1. Introduction

Zinc oxide (ZnO), a common wide band gap (~3.37 eV) oxide semiconductor, is widely used in the textile industry,[1] sensors,[2] supercapacitors[3] and catalysis[4] owing to its easy synthesis, low cost and unique physicochemical properties. Zinc is also an essential trace element in body tissues, which actively participates in the metabolic process of proteins, nucleic acids, lipids, *etc.*, thus playing an indispensable role in health maintenance.[5] Consequently, it is crucial to develop and explore the specific roles of ZnO in the biomedical field, which serves as a novel zinc delivery agent. At present, as one of the safe drugs approved by the Food and Drug Administration (FDA),[6] biocompatible ZnO has received increasing attention in various directions of biomedical research, including anti-inflammatory,[7] antibacterial,[8] anti-cancer,[9] drug delivery,[10] bioimaging,[11] gene therapy[12] and tissue regeneration.[13,14]

With the deepening of research, the single biomaterial treatment modality based on ZnO-based nanomaterials has been unable to satisfy the requirements of biomedical applications. In view of this, researchers began to construct a series of stimuli-responsive systems around ZnO-based nanomaterials according to the characteristics and difficulties of disease therapy. Stimuli-responsive materials are a class of smart materials that can respond to exogenous and endogenous stimuli, in which exogenous stimuli consist of light, ultrasound, magnetic fields, electric fields, pressure, *etc.*, while endogenous stimuli include temperature, humidity and so on.[15] This kind of smart material is sensitive to external environmental signals or pathological abnormalities, which can convert external stimuli into changes in its own dynamic structure or shape through various ways, thereby obtaining other unique physical or chemical properties, and exhibiting corresponding specific functions.[16] Recently, the system constructed by combining stimuli-responsive materials with extraordinary triggers has effectively achieved on-demand switching of treatment modes and reconciled the conflict between biocompatibility and therapy, which has shown great application potential in the fields of antibacterial, drug delivery, medical diagnosis and tissue engineering.[17,18] Nevertheless, although

[a]*School of Chemistry and Chemical Engineering, Nanchang University, Nanchang, Jiangxi, 330088, P. R. China. E-mail: wangxiaolei@ncu.edu.cn*
[b]*The Affiliated Stomatological Hospital, Nanchang University, Nanchang, Jiangxi, 330006, P. R. China*
[c]*The National Engineering Research Center for Bioengineering Drugs and the Technologies, Institute of Translational Medicine, Nanchang University, Nanchang, Jiangxi, 330088, P. R. China*

some stimuli-responsive ZnO-based materials have been reviewed,[19,20] they are mainly concentrated in a single stimulus or application, and few studies have systematically summarized or classified this material. Furthermore, there are fewer reviews on stimulus-responsive ZnO-based nanomaterials extensively studied for biomedical applications according to various stimulus sources.

This review focuses on the varying stimuli-responsive strategies of ZnO-based biomaterials, including exogenous stimuli (light, ultrasound, mechanical force, *etc.*) and endogenous stimuli (pH, enzymes, *etc.*) responsive strategies, and showcases the recent classical biomedical applications of ZnO-based biomaterials, such as antibacterial, anticancer, drug delivery and so on (Fig. 1). Firstly, the basic characteristics, response mechanisms and design principles of ZnO-based nanomaterials in response to a single stimulus are expounded, and a series of biomedical applications of such intelligent responsive systems in tissue repair, medical devices and therapeutic diagnostics are revealed. In addition, the constructions of multiple stimuli-responsive systems designed around ZnO-based nanomaterials are summarized, including two external stimuli-responsive strategies, as well as internal and external stimuli combined responsive strategies, while the biomedical applications of typical multi-responsive systems are enumerated. Finally, we also discuss the current challenges, improvement strategies and future prospects of stimuli-responsive ZnO-based biomaterials. The knowledge involved in this review may be conducive to constructing futuristic multifunctional biomaterials and designing corresponding intelligent responsive systems to meet the needs of a variety of disease diagnosis and treatment.

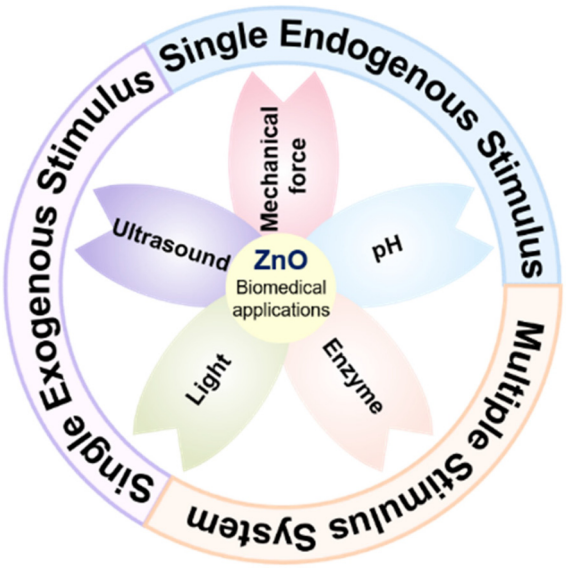

Fig. 1 A basic classification of major stimulus responsive systems associated with ZnO-based nanomaterials in biomedical applications.

2. Design and biomedical applications of single exogenous stimuli-responsive ZnO-based materials

ZnO-based materials play an important role as chemical sensitizers, which can intelligently respond to the corresponding changes in the external environment when exposed to exogenous stimuli, thus exerting specific functions in biomedical application research.[21] Exogenous stimuli, including light, ultrasound, electricity, magnetic field and mechanical force, can supply certain external energy, thereout constructing a series of non-intrusive therapeutic methods, such as photodynamic therapy (PDT), photothermal therapy (PTT) and sonodynamic therapy (SDT).[22] In the research progress of biomedical applications, the treatment strategy triggered by external energy has attracted much attention due to its weak invasiveness, high controllability, low damage and appreciable curative effect. Latterly, researchers have constructed diverse exogenous stimuli-responsive systems based on various ZnO-based nanomaterials and applied them to the fields of anticancer,[23] antimicrobial,[24] biosensors[25] and tooth bleaching.[26]

2.1 Light-triggered therapy

Light, as an engaging external stimulus, is equivalent to a non-invasive, temporally or spatially controllable switch trigger, which is not limited by factors such as ionic strength, temperature and pH, playing a vital role in the design of personalized intelligent treatment platforms.[27] In consequence, light-responsive biomaterials are favored in the research of different stimuli-responsive smart materials, which are widely used in various domains of biomedicine, including biosensing, drug delivery, fluorescence imaging, tissue repair and cancer therapy.[28–30] After the photosensitizer contained in the photoresponsive material is excited by light, the optical signal is converted into a physicochemical signal through the photochemical reaction process, so that the photosensitive material acquires homologous physical and chemical properties.[31] Among them, ZnO nanoparticles (ZnO NPs), the third generation of photosensitizers,[32] are important semiconductors with fascinating light response characteristics, which lay the foundation for designing safe and controllable therapeutic (or diagnostic) systems for many biomedical applications.

2.1.1 Photodynamic therapy. The expected curative effect of phototherapy systems based on ZnO-based nanomaterials is mainly achieved by PDT and PTT. In 2010, Kleinsasser *et al.*[33] first put forward the use of ZnO NPs for PDT, reporting that ZnO NPs in combination with the illuminant ultraviolet A (UVA-1, 340–400 nm) significantly reduced the viability of human head and neck squamous cell carcinoma (HNSCC) cell lines utilizing the photocatalytic effect. At present, the photocatalytic activity of ZnO NPs has been demonstrated by numerous studies, showing bright applications in antibiosis, anticancer and pigment degradation.[34–36] Additionally, ZnO NPs with a wide bandgap (~3.37 eV), which have strong ultraviolet (UV) absorption, are

also generally applied to the development of personal care products such as cosmetics and sunscreens.[37,38] However, the UV light signal tends to be attenuated with the absorption of tissue corona, which is not conducive to the diagnosis and treatment of diseases. Moreover, the long-term excessive action of UV light on the human body often causes certain damage to the eyes and skin,[39] which greatly limits the application of ZnO NPs. Therefore, how to utilize safer long-wavelength visible light and even infrared light energy is a prerequisite for biomedical research, while ensuring the biosafety of ZnO NPs.

Based on this, many studies have reported effective means to improve the defect that ZnO can only utilize radiation in the near UV region (Table 1). For example, only the surface chemical processing of ZnO is carried out to narrow the band gap of ZnO by introducing defects.[40] In addition, it also involves reducing the band gap by doping (non-metal, metal elements, *etc.*),[41–43] recombination (metal, non-metal, *etc.*),[44–46] hybridization (MOFs, UCNPs, *etc.*),[47,48] coupling narrow band gap materials[49] and developing oxygen vacancies,[50] thereby broadening the light absorption range.[51–54] Among them, Bahadur *et al.*[55] triumphantly synthesized copper (Cu)-substituted ZnO nanoassemblies (Cu-ZnO NAs) excited by visible light in 2017. It was found that the substitution of Cu ions could remarkably improve the light absorption properties, charge separation efficiency and reactive oxygen species (ROS) levels, which in turn enhanced the photosensitivity for sustained antibacterial and anticancer activity under dark and visible-light irradiation conditions. At the same time, it was demonstrated that Cu–ZnO NAs had a higher surface area to offer a mass of active sites, which facilitated the reinforcement of the photodynamic effect (Fig. 2A). In addition, Lai *et al.*[48] recently modified a zinc-based zeolitic-imidazolate framework (ZIF-8) on the surface of ZnO to form a core–shell structure (ZnO@ZIF-8) by traditional precipitation and hydrothermal methods. Compared with pure ZnO, the photocatalytic inactivation efficiency of ZnO@ZIF-8 under visible light excitation was markedly improved, which achieved coordinated antimicrobial

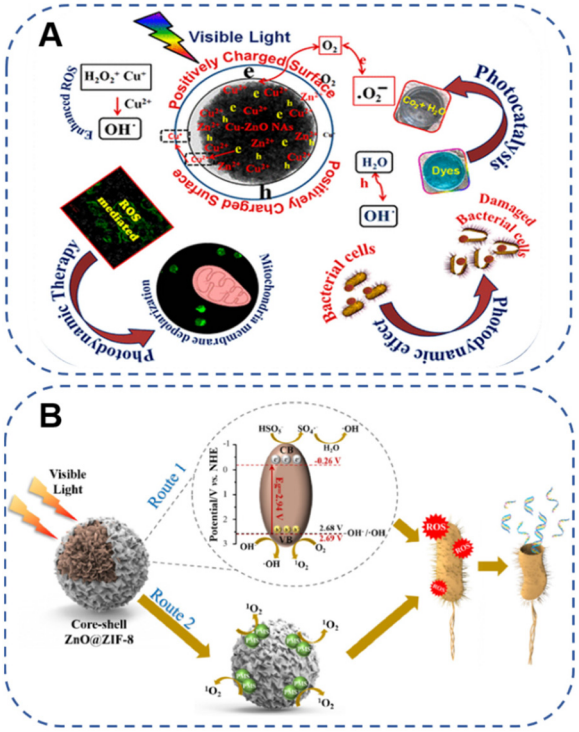

Fig. 2 (A) A new strategy to induce a photodynamic effect utilizing Cu–ZnO NAs under visible light excitation. Adapted with permission from ref. 55, copyright 2017, American Chemical Society. (B) Schematic diagram of the bacterial inactivation mechanism of PMS/ZnO@ZIF-8 with visible light irradiation. Adapted with permission from ref. 48, copyright 2022, Elsevier.

effects with peroxymonosulfate (PMS). Subsequent analysis of the mechanism of photocatalytic performance enhancement suggested that the core–shell structure of ZnO@ZIF-8 enabled the photogenerated holes to have better charge separation efficiency and stronger oxidation ability, further strengthening its bacterial inactivation effect (Fig. 2B). A great deal of research indicated that compared with traditional antibiotics,

Table 1 Construction of some representative narrow bandgap ZnO-based nanomaterials

Materials	Band gap	Light source	Mechanism	Ref.
ZnO NPs	3.28 eV	UV (368–378 nm)	Increase in crystallinity after high temperature calcination	51
NC-ZnO	3.12 eV	Visible light (>400 nm)	Doping nitrogen-doped carbon (NC) derived from ZIF-8 suppresses the recombination of e^- and h^+	41
m-ZnO	3.05 eV	Visible light (400, 555 and 665 nm)	Enhancement of oxygen vacancies	50
Tourmaline@ZnO	2.96–3.05 eV	Visible light (>400 nm)	Limiting the recombination rate of electron–hole pairs and improving the charge transfer efficiency at the interface	52
N-ZnO	2.99–3.04 eV	Visible light (≥400 nm)	Generation of new electronic states located between the valence and conduction bands due to the introduction of N atoms	42
ZnO@ZIF-8	2.94 eV	Visible light (≥400 nm)	Higher charge separation efficiency	48
g-C_3N_4/ZnO	2.82 eV	Visible light (400–800 nm)	Facilitating the separation of photogenerated e^- and h^+	43
p-Cu_2O/n-ZnO	2.11–2.14 eV	Visible light (>400 nm)	Promoting the efficient separation of photogenic carriers	53
ZnO@CdS	1.67 eV	Sunlight	Synergistic effect and shift of transmittance edges to lower regions	46
Zn_2GeO_4	1.25 eV	Air mass 1.5 (300–680 nm)	The interaction between O 2p and Ge 3d states near the Fermi level	54

visible light-responsive photocatalytic materials could eliminate infection and inflammation in a short time, with better controllability as well as less adverse reactions, which were less likely to induce drug resistance.[41] In other words, the development of photocatalytic antibacterial materials is an effective strategy to decrease the misuse of antibiotics.

In view of this, a series of novel porous ZnO composites with high specific surface area and narrow band gap (the narrowest band gap was 1.9 eV) were prepared by a simple microwave-induced method, and the corresponding material formative mechanism was discussed for the first time.[26] Because of the introduction of carbon, the synthesized ZnO composites could be excited by long-wavelength yellow light instead of harmful short-wave radiation, which exhibited efficient photocatalysis under the irradiation of yellow light, thereby radically improving the biosafety of ZnO photocatalytic applications. In the follow-up research works, aiming at a narrow band gap and high biosafety yellow light responsiveness, a variety of ZnO-based nanomaterials were systematically constructed, and their antibacterial applications in implant infection,[56] tissue reconstruction,[57] dental protective agent[58] and hearing protection[59] were explored respectively. Additionally, terbium doped ZnO (ZT, 2.4 eV) with green light response performance was also developed, which was modified with polydopamine coating and loaded with nitric oxide (NO) precursor drug *N*,*N*′-Di-*sec*-butyl-*N*,*N*′-dinitroso-1,4-phenylenediamine (BNN6) to prepare ZT@P@B nanoparticles for the modification of contact lenses.[60] Related experiments testified that the ROS formed by ZT with the assistance of green light could offer a satisfactory therapeutic window, fully exerting the photodynamic bactericidal effect. Of particular importance, under the irradiation of 808 nm near-infrared (NIR), the photothermal reaction mediated by polydopamine could achieve *in situ* release of NO, further enhancing the antibacterial properties while regulating the expression of related inflammatory factors, which was propitious to the improvement of bacterial keratitis. In conclusion, visible light driven ZnO-based photosensitizers are recognized for their potential usage in various biomedical applications. It is worth noting that the light source mentioned for the PDT of ZnO-based nanomaterials is not only restricted to visible light, but the research on ZnO-PDT treatment systems mediated by infrared light is also thriving. Taking the research work of Wu's group as an example,[61] they prepared an antimicrobial dressing with bacterial capture performance and short-term high antibiosis activity, namely the AgNPs/N-CD@ZnO xerogel. Encouragingly, its excellent antimicrobial activity was dependent on 808 nm NIR mediated PDT of ZnO NPs. In this study, N-CD@ZnO nanomaterials were synthesized by doping N-doped carbon dots (N-CDs), and it was found that after ZnO NPs were decorated by N-CD, the photodynamic response region was transferred from the original UV region to the 808 nm NIR region by up-conversion technology, indicating that N-CD@ZnO was a reliable upconversion material. As mentioned above, many researchers have reported visible/NIR mediated PDT of ZnO-based nanomaterials for antimicrobial infection, inflammation regulation and antitumor therapy.[62–64]

2.1.2 Photothermal therapy. PTT means that photothermal agents absorb light and convert it into heat under the illumination of light at a specific wavelength,[65] which can cause protein denaturation, cellular cavitation and rupture, *etc.*, leading to thermal ablation of needless cells at the target site. Based on the superiorities of high inherent specificity and low invasive burden, PTT emerges as an attractive and promising local heating strategy. Therefore, PTT constructed around ZnO-based nanomaterials provides new opportunities for the therapeutic of diseases such as microbial infection, inflammation and tumors. All along, the infrared phototherapy system based on ZnO NPs has attracted extensive attention from biomedical experts due to its safety controllability, strong tissue penetrability and standout antibacterial activity.[66] In 2017, as confirmed by Kannan *et al.*,[67] they found doxorubicin (DOX) supported polyethylene glycol (PEG) functionalized folic acid (FA) conjugated ZnO-NS (DOX-FA-PEG-ZnO NS), which could be regarded as a bifunctional carrier for photothermal chemotherapy of breast cancer. Among them, an FA molecule covalently bonded to ZnO-PEG could effectively target the FA receptor, thus achieving specific targeted drug delivery. Both *in vitro* and *in vivo* experiments bore out that the platform specifically delivered heat and drugs to the tumorigenic region under 808 nm NIR irradiation, thereby performing targeted chemophotothermal ablation of breast cancer cells. At the same time, the possible reasons for the absorption of DOX-FA-PEG-ZnO NS at 808 nm NIR were explained, mainly including the following two points. On the one hand, folate-conjugation on PEG-ZnO NS strengthened the 808 nm NIR absorbance, which might be attributed to the decentralized enhancement of ZnO NS solution and the further reduction of ZnO NS during the PEG functionalization. On the other hand, PEGylation and peptide modification could enhance the NIR absorbance, so the folate-functionalized PEG-ZnO NS also displayed a similar trend. Briefly, the constructed DOX-FA-PEG-ZnO NS was a breast cancer treatment system with advanced chemical photothermal synergistic targeted therapy performance and good drug release characteristics, which could effectively avoid frequent and invasive administration, further improving patient compliance.

Moreover, PTT is an effective and hopeful antibacterial means. For eradication of pathogenic bacterial infections, a novel NIR-triggered antibacterial platform based on a thermo-responsive polymer (TRB-ZnO@G) of MOF-derived 2D-carbon nanosheets (2D-CN) was reported in 2019.[68] The results indicated that the system possessed flexible 2D nanostructures, high photothermal activity, sustained zinc ions (Zn^{2+}) release and phase-size switching capability, which facilitated local clearance of multiple bacteria and enhanced anti-infective therapy (Fig. 3A). Recently, Wang *et al.*[69] deposited a photothermal multifunctional composite coating, namely Ti-PDA/BP/ZnO, on a titanium (Ti) substrate to design an anti-biofilm phototherapy platform with high thermal support for antimicrobial capability. The designed antimicrobial coating not only displayed good photothermal conversion ability under 808 nm NIR

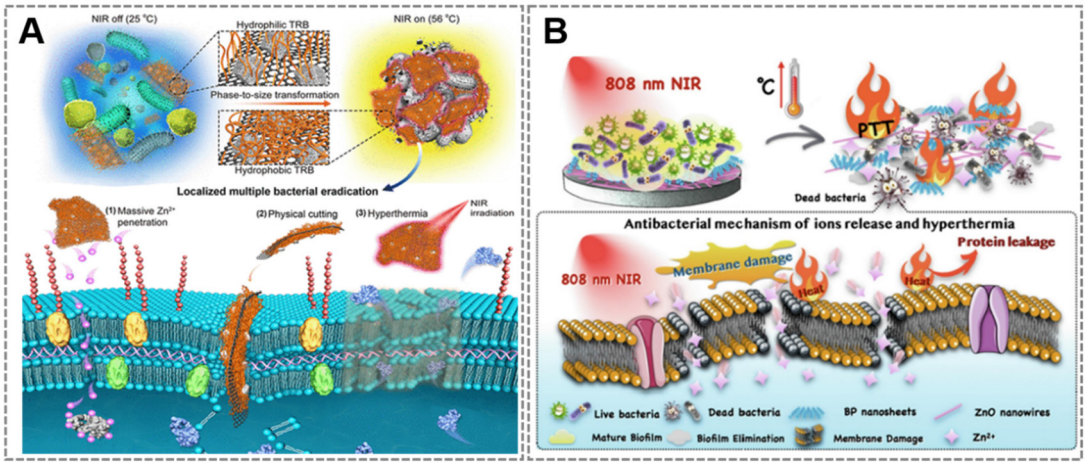

Fig. 3 (A) Sustained and topical triple antibacterial activity of the proposed TRB-ZnO@G, including chemical, mechanical and photothermal sterilization. Adapted with permission from ref. 68, copyright 2019, American Chemical Society. (B) Schematic illustration of the NIR triggered synergistic antibacterial activity of Ti-PDA/BP/ZnO coatings. Adapted with permission from ref. 69, copyright 2022, Elsevier.

irradiation, but also increased the susceptibility of bacteria to Zn^{2+} to obtain dramatic bactericidal performance, while accelerating the destruction of *Staphylococcus aureus* and *Escherichia coli* biofilms (Fig. 3B). Wherefore, the NIR triggered ZnO-PTT synergistic antibacterial strategy offered a conducive idea for *in situ* anti-biofilm adhesion of medical implant coatings, which also opened up new possibilities for the prevention and treatment of clinical implant infections.

2.1.3 Photodynamic and photothermal synergistic therapy. PDT combined with PTT has better clinical application potential than PDT or PTT alone, which is mainly attributed to two points. On the one hand, pure PDT requires abundant ROS to complete the therapeutic effect, while excessive ROS can cause normal tissue damage.[70] On the other hand, high temperature is indispensable for single PTT to achieve efficacy, which may be too high to ensure the survival of surrounding normal tissue.[71,72] Consequently, the application of PDT or PTT alone still has considerable limitations, and it is a feasible solution to construct synergistic treatment integrating PTT and PDT. In recent years, Professor Wu and his collaborators[73] presented a synergistic sterilization method of solar-mediated photodynamic and photothermal effects in 2019, and developed a red phosphorus (RP)/ZnO heterojunction film. For one thing, effective interfacial charge transfer and the improved separation efficiency of photogenerated electron–hole pairs could greatly promote the generation of ROS, which was helpful for photocatalytic disinfection. For another, RP/ZnO heterojunction revealed excellent solar photothermal conversion efficiency, thereby accelerating the eradication of *Escherichia coli* and *Staphylococcus aureus* through high temperature. In the same year, researchers embedded carbon quantum dots (CQD) modified ZnO (C/ZnO) into polydopamine (PDA) and FA to rapidly assemble an injectable hydrogel, called DFT-C/ZnO-hydrogel, for PDT combined PTT of infected wounds (Fig. 4).[74] The photothermal and photodynamic properties of the hydrogel were investigated, suggesting that the temperature of the DFT-C/ZnO-hydrogel could be increased to 55 °C under dual-light irradiation with wavelengths of 808 nm and 660 nm as shown in Fig. 4A. In contrast, the temperature of the DFT-hydrogel after double photoirradiation was much lower than 55 °C, which demonstrated that the higher photothermal effect of the DFT-C/ZnO-hydrogel was primarily ascribed to the presence of PDA and CQD. Subsequently, the strong photothermal effect and favorable photostability of the DFT-C/ZnO-hydrogel were further verified by switching experiments and infrared thermography, which pointed out that red light (660 nm) failed to induce the photothermal effect of the hydrogel (Fig. 4B–D). Besides, the photocatalytic activity of the hydrogel was investigated using the ROS fluorescent probe 2,7-dichlorodihydrofluorescein diacetate (DCFH-DA). The results confirmed that the hydrogel significantly enhanced the yield of ROS with 660 nm light irradiation, mainly because CQD could convert long-wavelength light to short-wavelength light, further resulting in the photoexcitation of ZnO and the generation of electron–hole pairs, which was beneficial to accelerate the generation of ROS (Fig. 4E). Finally, the results of *in vitro* and *in vivo* experiments demonstrated that DFT-C/ZnO-hydrogel combined with 660 nm and 808 nm dual-light treatment exhibited excellent photodynamic and photothermal antibacterial performance, which was suitable for application in infected wound healing. Afterwards, for the prevention and treatment of peri-implant diseases, our research group also adopted a two-pronged treatment measure of PDT and PTT, and constructed a tremella-like ZnO-adsorbed collagen type I (TreZnO@Col-I) coating for Ti surface modification.[56] Here, tremella-like ZnO (2.125 eV) acted as a photodynamic component and showed a good photocatalytic effect under yellow light (583 nm) stimulation, which could display broad-spectrum antibacterial activity, including against *Staphylococcus aureus*, *Escherichia coli* and oral-specific flora-variation *Streptococcus mutans*. In addition, the system possessed stable photothermal conversion properties and generated a local

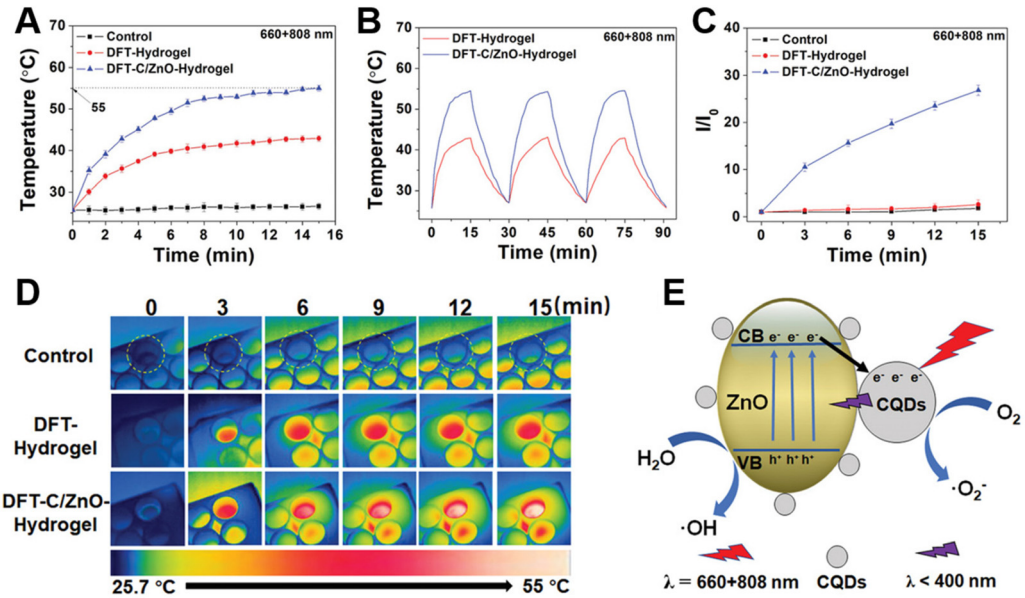

Fig. 4 Photothermal and photodynamic properties of hydrogels. (A) Photothermal curves of the hydrogel under 15 min light irradiation (660 nm and 808 nm). (B) Temperature rising and cooling curves of the hydrogel with 660 nm red light and 808 nm NIR irradiation. (C) Real-time infrared thermal images of different hydrogels immersed in PBS aqueous solution under light illumination at 660 nm and 808 nm. (D) Fluorescence intensity (FI) at 525 nm after immersion in fluorescent dye solution and irradiation with light. I_0: FI of the initial value, I: FI of different times. (E) Schematic diagram of the photothermal and photodynamic performance process of hydrogels under mixed light. Adapted with permission from ref. 74, copyright 2022, Wiley.

hyperthermal microenvironment beneficial for osteogenesis under 808 nm NIR excitation.

Although PDT and PTT based on ZnO nanomaterials have been widely used in various aspects of the biomedical field (Table 2), there are still potential limitations to be broken through in existing phototherapy strategies. In the case of PDT, the photosensitizer absorbs light energy and transfers it to oxygen, which leads to the generation of energy-state transitions, thereby increasing the production of ROS such as singlet oxygen ($^1O_2$).[75] In addition to light sources and photosensitizers, oxygen is an indispensable part of the PDT process. However, hypoxic conditions, such as in tumor site[76] and bacterial infection microenvironments,[77] severely inhibit the efficacy of PDT. In order to alleviate the hypoxia, a number of oxygen-producing materials (nanozymes, hydrogel, microalgae, *etc.*) have been developed, but they are inactive due to the acidic environment of the lesions.[78] Besides, the mitochondrial respiration of related cells is relatively active, which consumes a part of the oxygen, further increasing the difficulty of improving the hypoxic environment.[79] Hence, it is necessary to optimize the existing oxygen supply materials or develop new photosensitizers from the perspective of continuous oxygen production and inhibition of oxygen consumption.

2.2 Ultrasound-triggered therapy

Despite the advantages of light as described above, its poor penetration into tissue hinders further applications. On the contrary, ultrasound with high tissue penetration overcomes

Table 2 Summary of the representative biomedical applications of ZnO-based nanomaterial phototherapy

Materials	Light source	Phototherapy strategy	Application field	Ref.
LCL/ZnO	Chemiluminescence of luminol (~660 nm)	PDT	Antitumor	64
CEP-Ag@AgCl/ZnO	Visible light (>420 nm)	PDT	Antibacterial	63
ZnO/BiOBr	Visible light (>400 nm)	PDT	Antibacterial	62
ZnO/UCNPs	808 nm NIR	PDT	Antibacterial	47
AgNPs/N-CD@ZnO	808 nm NIR	PDT	Bacteria-infected wounds	61
t-ZnO	527 nm green light	PDT	Wound healing	40
DOX-FA-PEG-ZnO NS	808 nm NIR	PTT	Anti-breast cancer	67
ZnO@PDA-DOX/DZ	808 nm NIR	PTT	Antitumor	66
Ti-PDA/BP/ZnO	808 nm NIR	PTT	Implant infections	69
TRB-ZnO@G	808 nm NIR	PTT	Anti-infective	68
RP/ZnO	Solar light	PDT/PTT	Antibacterial	73
DFT-C/ZnO-hydrogel	660 nm red light and 808 nm NIR	PDT/PTT	Wound healing	74
Ti-ZnO@Col-I	583 nm yellow light and 808 nm NIR	PDT/PTT	Peri-implant diseases	56

the critical problem of penetration depth limitation, making it possible to monitor and treat deep diseases.[80] Studies have shown that ZnO NPs are ideal biocompatible ultrasound contrast agents. For instance, a novel type of implantable passive sensor for mechanical properties of biological tissues was constructed by embedding ZnO NPs into polydimethylacrylamide nanocomposite hydrogels, which was able to operate with large linear ultrasonic sensitivity and cover the strain monitoring of soft tissue and hard tissue, realizing remote assessment of organ deformation after implantation.[81] Furthermore, ultrasound has the advantages of clinical safety, non-invasiveness as well as high selectivity, and the customized diagnosis and treatment platform constructed by ultrasound shows gigantic application potential in the fields of drug delivery, biological imaging and disease treatment.[82] The treatment method using the synergistic effect of ultrasound and a sonosensitizer is called SDT.[83] The major principle is to utilize low-intensity (0.5–4.0 W cm^{-2}) ultrasound to irradiate the lesion location of the enriched sonosensitizer, which can *in situ* activate the sonosensitizer to generate toxic ROS, including superoxide anions ($^{\bullet}O_2^-$), hydroxyl radicals ($^{\bullet}OH$) and $^1O_2$, so as to enable site-specific disease treatment. So far, correlation research studies have shown that the possible mechanism of SDT to produce ROS is mainly the ultrasonic cavitation effect.[84] The cavitation effects induced by ultrasound include stable cavitation generated by the continuous oscillation of microbubbles, as well as inertial cavitation caused by rapid growth and rupture of microbubbles, which is closely related to the generation of ROS. Inertial cavitation can induce hydrothermal dissociation to generate ROS, namely $^{\bullet}OH$. Additionally, the sonoluminescence phenomenon invoked by cavitation is to excite the electron orbital of the sonosensitizer by transferring energy, and promote the production of ROS when the excited electrons return to the ground state, while the increase of the ROS concentration in the body depends on the structure of the sonosensitizer.[85]

Compared with conventional therapies, SDT, a hopeful non-invasive treatment technique, is implemented to target precisely the lesion location through the selection and modification of sonosensitizers, which leads to apoptosis of pathological cells, as well as less damage to normal cells and tissues.[86] It is noteworthy that the selection of sonosensitizers is one of the key links in achieving effective SDT. The ideal sonosensitizer should have good biosafety, precise aggregation targeting, high stability in specific environments and strong sensitivity to ultrasound. Currently, the commonly used sonosensitizers are mostly organic sonosensitizers,[87,88] such as hematoporphyrin, phthalocyanine, DOX, *etc.*, most of which have poor biocompatibility, low water solubility, weak chemical stability, and short blood circulation time which cannot effectively accumulate at the disease site, making SDT ineffective. In view of this, researchers have successively synthesized inorganic nanomaterials[89] with the characteristics of sonosensitizers, which contain the advantages of distinctive energy level structure, good chemical stability and high concentration at the lesion site compared with organic sonosensitizers, making them widely used in SDT. Among them, inorganic semiconductor sonosensitizers represented by ZnO NPs[90,91] and titanium dioxide nanoparticles[92,93] have received extensive attention. In the early years, Webster *et al.*[94] demonstrated that ZnO NPs exhibited superior antibacterial properties against *Staphylococcus aureus*, which further enhanced its bactericidal activity in the presence of ultrasound, expecting to be used for the anti-infection of medical devices. Similarly, Bahadur *et al.*[95] selected ultrasound as an *in vitro* stimulus source for smart drug carriers based on porous ZnO NPs. They verified that ultrasound could cause extreme changes in the temperature and pressure of the interface between the anticancer drug DOX as well as ZnO NPs through the cavitation mechanism within a short period of time, which facilitated drug detachment from the carrier, thereby reinforcing controlled and targeted on-demand drug delivery. Unfortunately, pure wide-bandgap ZnO NPs as inorganic sonosensitizers suffer from low yields of ROS (*e.g.*, $^1O_2$ and $^{\bullet}OH$) under ultrasound activation due to the fast recombination rate of electrons (e^-) and holes (h^+),[96] so the therapeutic effect is not evident. Furthermore, a low specific surface area is also a significant factor limiting ultrasonic sensitivity and leading to poor acoustic dynamics, because a high specific surface area is conducive to enhancing the ultrasonic cavitation effect to release higher energy.[97] In consequence, how to design an ideal ZnO-based nanomaterial sonosensitizer with biocompatibility and dramatic sonodynamic therapeutic efficiency has become a challenging research topic.

Based on the above problems, researchers have adopted effective strategies such as biochar loading,[98] metal doping[99] and defect engineering[100] to tune the electronic structure, band gap, specific surface area as well as the catalytic performance of ZnO NPs. For instance, Shim *et al.*[101] reported a new means to construct piezoelectric nanohybrids (Au@P-ZnO NRs) for chemical piezoelectric catalytic tumor therapy by incorporating gold nanoparticles (Au NPs) to heighten the piezoelectric catalytic activity of ZnO NRs and loading the pro-oxidant anticancer drug piperlongumine. The finding manifested that the deposition of Au NPs could significantly increase the piezoelectric catalysis of ZnO NRs, further enhancing ROS formation (Fig. 5A). Furthermore, *in vitro* and *in vivo* experimental results demonstrated the feasibility of piezoelectric nanohybrids (Au@P-ZnO NRs) to realize ultrasound-triggered piezoelectric catalytic cancer therapy combined with cancer-specific chemotherapy. In an outstanding work, Professor Zhang's group[100] improved the performance of ZnO-SDT by adjusting electron transport through defect engineering, synthesizing a novel sonosensitizer, defect-rich gadolinium (Gd) doped ZnO nanospheres (D-ZnOx:Gd), which overcame the difficulty of low quantum yield of ROS produced by pure ZnO NPs. Compared with the defect-free ZnO NPs, the abundant oxygen-deficient sites of D-ZnOx:Gd could supply electron capture sites, which was beneficial to boost the separation of e^- and h^+ from the energy band structure after ultrasonic irradiation, thus evidently strengthening the sonodynamic effect. Meanwhile, the defect-rich D-ZnOx:Gd more

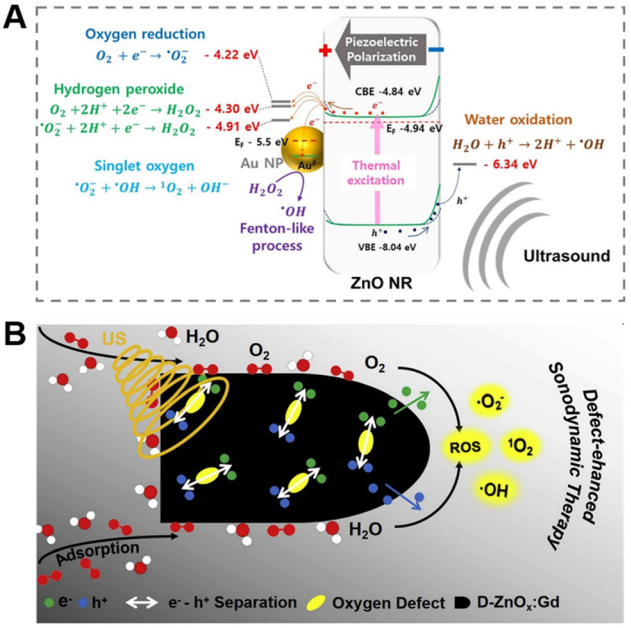

Fig. 5 (A) Piezoelectric catalytic mechanism of Au@P-ZnO NRs. Adapted with permission from ref. 101, copyright 2022, Elsevier. (B) Mechanism of ROS generation from defect-rich D-ZnOx:Gd. Adapted with permission from ref. 100, copyright 2020, Elsevier.

easily adsorbed oxygen and water molecules, which greatly enhanced the ability to generate ROS (Fig. 5B). The results certificated that the defect-rich D-ZnOx:Gd sonosensitizer obtained by defect engineering could produce a large amount of ROS regardless of tissue depth, thereby achieving high ultrasound-mediated killing efficiency of breast cancer cells. The ultrasonic responsive system of ZnO-based nanomaterials is favored by biomedical experts due to its clinical safety, non-invasiveness and high tissue penetration, while its defects to be improved also attract much attention. Likewise, SDT has analogous problems with PDT, where oxygen is an essential element of the SDT process. As such, how to build ZnO-based sonosensitizers that can generate oxygen deserves further exploration by researchers.

2.3 Mechanical force-triggered therapy

Mechanical force[102] is very common in biological systems and exists extensively in diverse forms of intrinsic involuntary or voluntary stimulation, including heartbeat, lung dilation, chewing, *etc.* Conversely, appropriate mechanical stimuli can also participate in biological activities, such as angiogenesis and bone regeneration, affecting multiple biomechanical processes.[103] Therefore, it is crucial to design and construct a mechanoresponsive nanoplatform for diagnosis and treatment. Piezoelectric materials,[104] a class of intelligent substances with piezoelectric properties, can convert mechanical energy into electrical energy under mechanical stimulation. Currently, a variety of piezoelectric materials have been explored for biomedical research, including piezoelectric inorganics, piezoelectric polymers and hybrid piezoelectric materials.[105,106] Among them, ZnO is a typical piezoelectric inorganic material, usually with extremely high piezoelectric coefficient and good mechanical properties, showing excellent application potential in the field of electroactive tissue repair.[107] Based on this, related researchers have prepared a series of therapeutic platforms endowed with mechanical response functions based on ZnO NPs, comprising tissue engineering scaffolds,[108,109] composite material coatings,[110] piezoelectric dermal patches,[111] *etc.* Their effects on angiogenesis, wound healing and bone tissue formation were also explored.

Numerous studies have indicated that electrical stimulation generated by piezoelectric materials can modulate the activity of associated cells such as cardiomyocytes, osteoblasts and neural cells, while affecting cellular processes including proliferation, migration as well as differentiation.[112,113] For example, Murillo *et al.*[114] chose a two-dimensional ZnO nanosheet network as a piezoelectric nanogenerator, which could respond to the intrinsic force generated by cells and induce local electric field stimulation, thereby promoting the proliferation and differentiation of macrophages and human osteosarcoma cells (Saos-2). On this basis, researchers modified a ZnO nanosheet coating on the surface of a Ti-based alloy ($Ti_{45}Zr_{15}Pd_{30}Si_5Nb_5$) to induce electrical self-stimulation of osteoblasts, while avoiding the use of silicon.[110] Besides, in terms of nerve repair, Zheng *et al.*[113] loaded ZnO into polycaprolactone (PCL), a commonly used material for nerve conduit manufacturing, and fabricated ZnO/PCL piezoelectric nanogenerator scaffolds by means of 3D injectable multilayer biofabrication technology. Subsequently, the effect of the ZnO/PCL scaffold on the viability of Schwann cells was investigated, which suggested that the ZnO/PCL scaffold had low toxicity similar to the PCL scaffold (Fig. 6A), and the oxidative stress produced by the ZnO/PCL scaffold was also comparable to that on the PCL scaffold (Fig. 6B and C). Next, the morphology and adhesion of Schwann cells on the two scaffolds were also observed, which concluded that the electrical signals generated by the ZnO-loaded scaffolds stimulated protrusion extension and increased cell adhesion to the material interface (Fig. 6D–I). Finally, it was verified that physical exercise was selected as a simulation of external mechanical signals to trigger the ZnO/PCL scaffold to produce a bioelectric environment, when rats exercised on a treadmill. The unique approach not only speeded up nerve conduction, but also promoted axonal myelination, ultimately restoring motor function by repairing endplate muscles. In conclusion, the mechano-informative biomimetic piezoelectric scaffold designed by the authors provided a new perspective for nerve repair and might have great application potential in the neural engineering of regenerative medicine.

Moreover, the piezoelectric effect endows ZnO-based nanomaterials with more promising antibacterial and healing properties.[115] To accomplish spontaneous wound healing, Kim *et al.*[111] developed a ZnO nanorod piezoelectric patch (PZP) based on bidirectional growth by using the characteristic. It was found that piezoelectric materials could generate endogen-

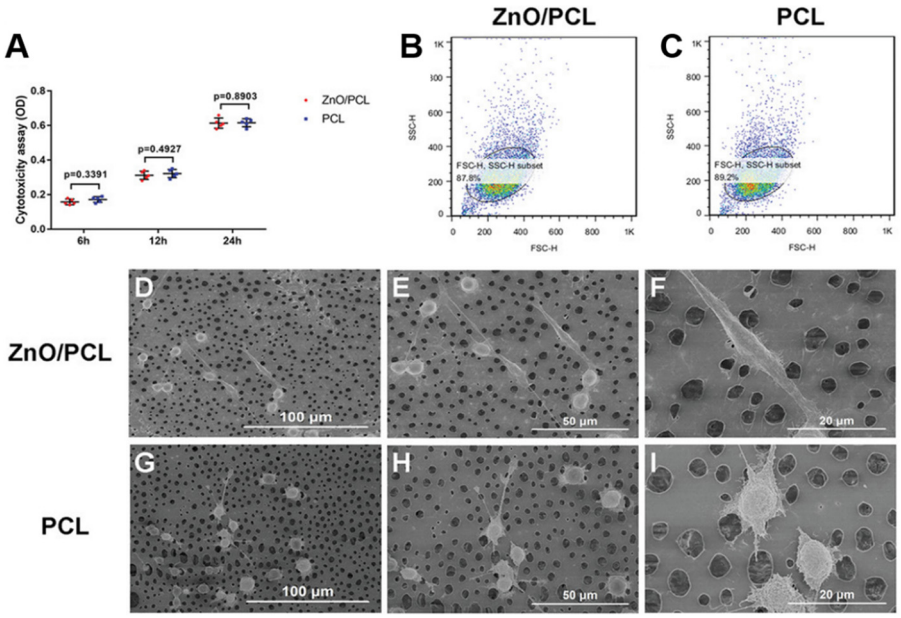

Fig. 6 (A) Cytotoxicity assay of Schwann cells seeded on 10% ZnO/PCL and PCL scaffolds. (B and C) Oxidative stress in Schwann cells on ZnO/PCL and PCL scaffolds. (D–F) Schwann cell morphology on ZnO/PCL scaffolds. (G–I) Schwann cells morphology on PCL scaffolds. Adapted with permission from ref. 113, copyright 2020, Wiley.

ous electric fields even under small mechanical deformation, avoiding the utilization of auxiliary external electrical equipment to induce endogenous electric fields. *In vitro* and *in vivo* experiments testified that the piezoelectric patch application supported an endogenous skin regeneration process on account of electrical stimulation, which accelerated wound healing by regulating inflammatory responses, promoting cellular regenerative activity, quickening neovascularization and enhancing tissue remodeling. For the treatment of infected wounds, Fan *et al.*[116] reported a novel bi-piezoresponse hydrogel scaffold, namely ZnO nanoparticle-modified polyvinylidene fluoride (PVDF)/sodium alginate (SA) piezoelectric hydrogel scaffold (ZPFSA), which rationally designed bi-piezoresponse properties including vertical and horizontal orientations, thus ensuring sustainable bioelectrical stimulation signals. The resulting bioelectric environment provided favorable conditions for activities related to wound healing, such as bacterial eradication, cell migration, collagen remodeling and vascularization. In summary, the unique work not only expanded the application of piezoelectric materials in wound dressings, but also offered an originative option for promoting rapid healing of infected wounds and preventing scarring.

It is worth mentioning that the source of mechanical stimulation of piezoelectric materials can also be provided by self-driving bacteria. *Bdellovibrio*,[117] a natural predator with activity, can move rapidly (160 m s^{-1}) by rotating unipolar flagella and hit its "prey", as well as killing the "prey" after entering its peripheral cytoplasm. Inspired by this, Professor Zhang and his collaborators[118] proposed a material-assisted microorganism (MAMO) strategy that introduced ZnO nanorods on the surface of predatory *Bdellovibrio* with high-speed collision capability to obtain ZnO-modified *Bdellovibrio*, namely ZnO@Bdello. The modified *Bdellovibrio* moved rapidly and collided with the biofilm, and the generated mechanical pressure induced ZnO polarization and produced a large amount of ROS, both of which had a synergistic antibacterial effect on the bacteria of the biofilm. Subsequently, the resistance of the system to biofilms and bacteria was verified in complex biofilm models including rat and rabbit periodontitis models. It was also found that ZnO@Bdello could not only destroy biofilms, but also reduce the abundance of periodontal pathogens to inhibit periodontitis without producing detectable pathogen resistance and side effects (Fig. 7). In addition to formulating the aforementioned disease treatment strategies, ZnO-based piezoelectric nanomaterials have also been generally applied to the construction of electronic skins, wearable devices and other applications related to disease diagnosis as well as health care, resulting in considerable progress.[119–121]

2.4 Other exogenous stimuli-triggered therapy

The microwave response behavior of ZnO NPs is another fundamental property for their biomedical applications due to their high exciton binding energy (~60 meV) and wide bandgap (~3.37 eV), which can absorb microwave energy and convert it into thermal energy, forming a local thermal effect.[122,123] Simultaneously, microwave irradiation is also an external stimulus with excellent penetrating performance and good controllability, while furnishing an excellent thermal effect.[124,125] Hence, microwaves have become one of the potential stimulus sources for ZnO-based intelligent materials. Wu *et al.*[126] synthesized mesoporous core–shell nanomaterials (Fe_3O_4@mZnO) by homogeneous precipitation, a highly drug-loaded drug carrier with

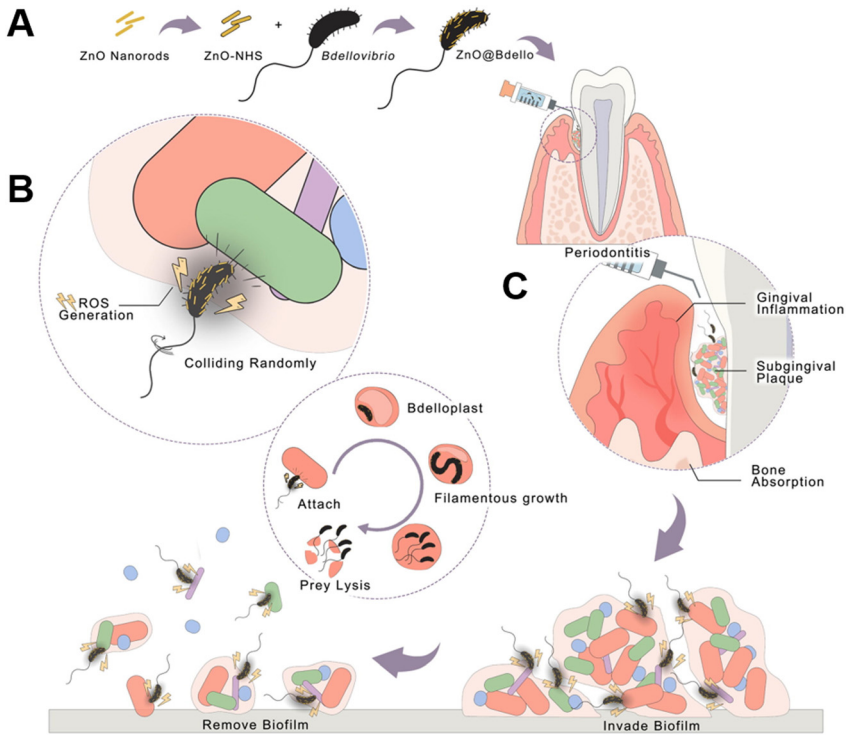

Fig. 7 Schematic illustration of ZnO@Bdello removal of the dental plaque biofilm. (A) Preparation of ZnO@Bdello. (B) The predation process of ZnO@Bdello. (C) In periodontitis, ZnO@Bdello invaded and removed subgingival biofilm, thereby inhibiting gingival inflammation and alveolar bone resorption. Adapted with permission from ref. 118, copyright 2022, Elsevier.

microwave-responsive and magnetic response properties, which was expected to be used for targeted delivery of drugs in combination with chemotherapy and microwave hyperthermia system construction. Furthermore, the magnetic response is also one of the stimulus sources of the ZnO-based responsive system, which has the special functions of controlling transmission, including telemanipulation and magnetic resonance imaging.[127] As previously mentioned, the magnetically responsive ZnO-based smart system enables on-demand and site-specific drug delivery.[126] In another study, Cauda *et al.*[128] suggested an approach to reinforce ZnO performance through iron doping to design a multifunctional theranostic nanoplatform for cancer cell therapy, namely Fe:ZnO NPs. In this system, Fe:ZnO NPs had biological imaging potential, which offered a new avenue for the development of intelligent disease diagnosis systems.

3. Design and biomedical applications of single endogenous stimuli-responsive ZnO-based materials

Endogenous signals can be highly disordered under pathological conditions, providing more possibilities for the construction of intelligent nanoplatforms for endogenous stimulus responses, which can be used to perform accurate and effective treatment by distinguishing healthy sites from diseased sites.[129] In addition to the previously reviewed combination of ZnO-based materials with exogenous stimuli such as light, ultrasound and mechanical force for the diagnosis and treatment of diseases, including cancer, inflammation and microbial infections, researchers have designed a series of endogenous stimuli-responsive ZnO-based materials.[130,131] The material can specifically respond to endogenous signals related to the microenvironment of the lesion site, such as pH, enzymes and glutathione, so as to ameliorate the defects and efficacy of existing therapies in biomedical applications containing drug delivery, disease diagnosis and disease treatment, which is expected to develop personalized treatment systems.

3.1 pH-triggered therapy

The pH is one of the biological parameters usually altered in characteristic disease states, such as tumors and microbial infections (acidic pH), so it is essential to develop a pH-responsive platform based on bioresponsive materials.[132] The design of pH responsive materials should satisfy the following requirements, that is, bioresponsive materials can dynamically change their structural properties, including swelling, contraction, dissociation and degradation, in the context of a pathological environment with low pH, thereby implementing particular bioactive molecule delivery and disease treatment.[133] ZnO NPs are pH-sensitive materials that are only stable under normal physiological conditions (pH 7.4), while in acidic conditions (pH < 5.5), the nanostructures incline to dissolve rapidly and release Zn^{2+},

which can be used for antiseptic and anticancer purposes.[134] Meantime, ZnO NPs with pH-triggered characteristics have also become potential candidates for convenient smart nanocarriers due to their simple design, tunable size and low toxicity, which can not only quickly achieve specific biodegradation, but also selectively release drugs. In 2010, ZnO NPs were first reported as a pH-responsive drug delivery system.[95,135] Since then, the class of materials has been rapidly developed and widely used in the delivery of various disease therapeutic drugs (Table 3). Other studies showed that after ZnO NPs dissolved in response to physiological and pathological pH signals, the generated Zn^{2+} exhibited obvious cytotoxic effects on cancer cells.[136]

ZnO quantum dots (ZnO QDs) are a popular drug carrier due to their small particle size and easy phagocytosis by cells.[137] ZnO QDs are mostly used as nanocarriers to convey antitumor drugs, such as DOX,[138] mitoxantrone hydrochloride,[139] 5-fluorouracil (5-FU)[140] and curcumin,[141,142] explaining that the pH-triggered intelligent drug-releasing anti-cancer system can further enhance the efficacy of cancer treatment through synergistic anti-tumor of Zn^{2+} and drugs. Zhu's team[137] and Feng's team[138] constructed a pH-responsive ZnO@MSN drug delivery system (DDS) loaded with DOX based on acid-decomposable ZnO QDs and mesoporous silica nanoparticles (MSN), respectively. In their systems, ZnO QDs acted as gatekeepers to block the nanopores of MSN, enabling "zero premature" drug release in the physiological environment. Finally, the effective combination of ZnO QDs that released Zn^{2+} triggered by acidic pH, and the anti-tumor drug DOX achieved a synergistic anti-tumor effect, raising the therapeutic index while reducing side effects. Regrettably, whether mesoporous silica can be biodegraded and excreted remains to be discussed.[143] Mesoporous carbon nanoparticles (MCN) have similar structural characteristics and properties to mesoporous silica, which show lower cytotoxicity than mesoporous silica, promising to replace mesoporous silica for the construction of drug delivery systems. Based on this, Du *et al.*[139] reported an MCN-based drug delivery system, the gated MCN drug delivery system (ZnO-gated MCN), in which ZnO QDs were also selected as the gatekeepers of the system. The surface of the carboxylated MCN was covalently connected to the carboxylated ZnO QDs through double amide bonds, which could not only improve the drug loading capacity, but also minimize the premature release of the drug. After loading the hydrophilic antitumor drug mitoxantrone hydrochloride (MIT-HCL), it exhibited about 65% high cytotoxicity to A549 cells even at a drug dose of 0.066 ng per cell, implying that the system had a prospective application in tumor treatment.

ZnO QDs, however, are prone to agglomeration, and the strong adsorption of mesoporous materials on drugs leads to incomplete drug release, which is where further improvements are needed for the type of drug delivery system.[144] In view of this, researchers successively exploited many modification methods of bare ZnO QDs, such as amino modification,[143] zwitterionic polymer P (CBMA-*co*-DMAEMA) modification,[145] gadolinium ion (Gd^{3+}) doping,[146] *etc.*, where the modified ZnO QDs were used as nanocarriers for carrying drugs.[147] Kong *et al.*[146] designed a novel pH-sensitive multifunctional composite nanoplatform by introducing polymer-coated ZnO QDs to compound gadolinium ions and adsorbing DOX, carrying out three functions of small animal fluorescence labeling, magnetic resonance imaging and drug release for tumor treatment, which was one of the representative works of diagnosis and treatment integration. In another study, it was also found that the construction of cluster-like ZnO QDs could improve their stability. For instance, an investigation by Lin *et al.*[148] demonstrated an instant pH-responsive drug-loaded nanocluster (PEG-cZnO-DOX) based on ZnO QDs, which was composed of small single ZnO QDs capped by cross-linking dicarboxyl-terminated polyethylene glycol (PEG), further loading with a large amount of DOX through complexation and covalent interaction. When placed in tumor cell endosomes, PEG-cZnO-DOX specifically responded to low pH, and the carrier was comple-

Table 3 Summary of pH-responsive ZnO-based materials for drug delivery

Drug-delivery systems	Drug	Cell type	Highlight	Ref.
DOX-loaded ZnO NSs	DOX	HepG-2, HeLa	Biodegradable, tumor accumulation, ultrasmall particles	149
HA-ZnO-PEG	DOX	A549	CD44-targetable, pH-responsive	143
PEG-cZnO-DOX	DOX	A549, MCF7	Fully biodegradable, tumor-specific accumulation, synergistic antitumor	148
ZnO/DOX	DOX	MDA-MB-231, HeLa, MES-SA/Dx5, NCI/ADR-RES	Specific targeting, multi-faceted anti-cancer	150
ZnO-DOX@HAase/PEG-PAH-DMMA	DOX	4T1	Enhanced tumor penetration and proximity effect	151
ZnO-Gd-DOX	DOX	BxPC-3	Fully biodegradable, bioimaging capabilities, no obvious side effects	146
ZnO@MSNs-DOX	DOX	HeLa	Prevents the cytotoxic drug from premature release	137
ZnO@MSN-K_{10}	DOX	HepG2	Dual pH-sensitive, escape from the endosomes	138
ZnO@P (CBMA-*co*-DMAEMA)	DOX	HepG2	Enhances water stability, increases blood circulation time, and promotes endocytosis	145
5-FU@ZIF-90@ZnO	5-FU	HeLa	High treatment efficiency, low drug toxicity, renal pathway excretion	140
ZnO-gated MCN	MIT	A549	Double amide bond covalently linked, high biocompatibility	139
ZnO-PBA-curcumin	Curcumin	MCF-7	Specific targeted delivery, tumor accumulation	142

tely dissolved while causing the metal-drug complex to be decomposed, thus realizing complete biodegradation and efficient drug release of the system. More importantly, the pH-responsive PEG-cZnO QDs cluster system with a size of about 70–80 nm could perform tumor homing and accumulation while circulating in the blood through enhanced permeability and retention effect, acting as a synergistic anti-tumor effect.

Besides, some studies have reported that appropriately sized ZnO NPs[140,141] or ZnO nanospheres (ZnO NSs) assembled from ultra-small particles[149] are also ideal pH-responsive drug carriers. As confirmed by Wang *et al.*,[149] the as-synthesized ZnO NSs assembled by ultra-small particles, with excellent properties such as being size-tunable, monodisperse and biodegradable, were used for DOX charging. The structure of the DOX-loaded ZnO NSs nanoplatform was destroyed in a weakly acidic environment, while releasing drugs and ultra-small nanoparticles to meet the requirements of pH-stimulated drug release, which was beneficial to biodegradation. *In vitro* cell experiments made clear that the system effectively reduced the cell viability of human hepatocellular carcinomas (HepG-2) and HeLa cells, showing a dose-dependent and time-dependent effect. Finally, *in vivo* experiments bore out that the DOX-loaded ZnO NSs system displayed significant anti-tumor effects, with an average inhibition rate of 79% relative to the control group, and no obvious side effects (Fig. 8). Related researchers have proposed that ZnO NPs can be a nanocarrier as well as the multi-target therapeutic agent.[150,151] Zhu's group[150] demonstrated for the first time that ZnO NPs could efficaciously target a variety of cells, including cancer cells, cancer stem cells and macrophages. It was mainly reflected in the fact that ZnO/Dox could be effectively internalized by both drug-sensitive and multidrug resistant cancer cells and penetrate more efficiently through three-dimensional (3D) cancer cell spheroids compared with free Dox. Moreover, ZnO NPs could efficaciously downregulate the key surface marker CD44 of cancer stem cells and decrease the stemness of cancer stem cells, thus improving the sensitivity of Dox therapy, inhibiting the adhesion and migration of cancer cells, and preventing the formation of tumors (3D cancer cell spheres). In addition, as immunomodulators, ZnO NPs could protect macrophages from Dox-induced toxicity and promote the Dox-induced macrophages to polarize toward an M1-like phenotype. Synchronously, ZnO NPs perform multiple key functions, such as inhibiting cancer proliferation, sensitizing drug-resistant cancers, preventing cancer recurrence and metastasis, as well as resuscitating cancer immune surveillance. Additionally, some functionalization strategies have been proved for the modification of ZnO NPs. For example, the researchers explored the pH response of phenylboronic acid (PBA)-functionalized ZnO NPs (~40 nm in diameter) for tumor tissue-specific delivery of curcumin (ZnO-PBA-curcumin).[142] PBA conjugation was found to facilitate the targeted delivery of curcumin, and the anticancer efficacy of the system could be attributed to the differential oxidative stress-inducing charac-

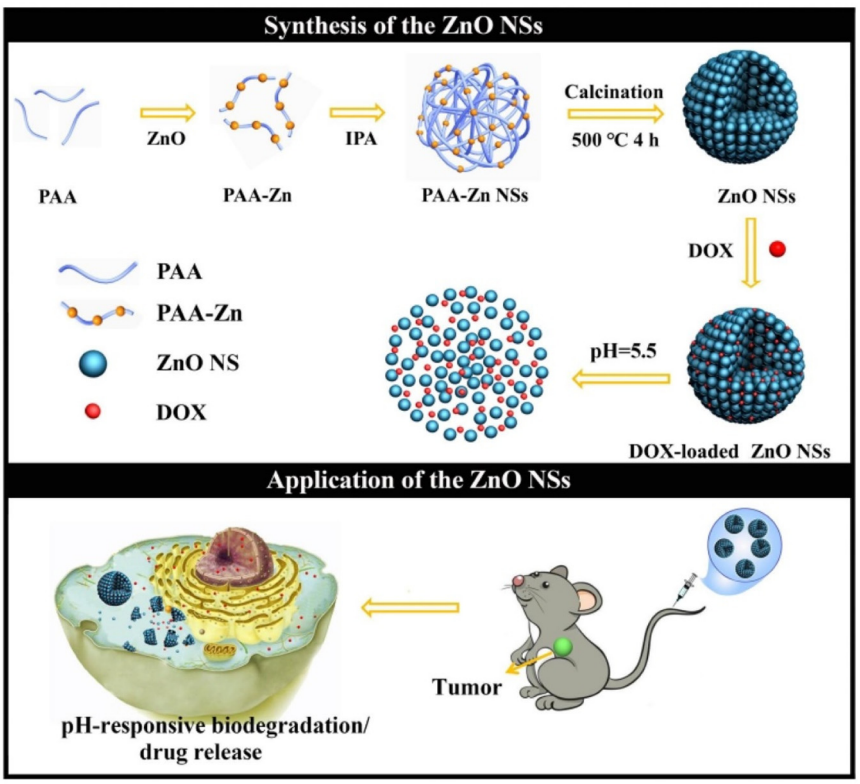

Fig. 8 Tunable synthesis of pH-responsive biodegradable ZnO NSs assembled by ultra-small particles for cancer chemotherapy. Adapted with permission from ref. 149, copyright 2019, Elsevier.

teristics of curcumin and Zn^{2+}, which afforded insights into the PBA-functionalized tumor cell targeting mechanism. Furthermore, Wang *et al.*[152] assembled a delicate self-catabolizing multifunctional DNAzyme nanosponge using ZnO NPs as stimulus-responsive DNAzyme cofactor precursors for programmable drug delivery and efficient gene silencing.

Besides constructing intelligent drug-loading systems, pH-responsive ZnO-based nanomaterials have also been applied to antibacterial, tissue regeneration and pneumonia treatment.[153,154] For example, Zhao *et al.*[153] developed pH-responsive Ber@ZnO-Z nanospheres, in which ZnO NSs and ZIF-8 acted as core–shell and shell (ZnO-Z), respectively, further encapsulating the fungicide berberine (Ber) in the core–shell ZnO-Z carrier. In this work, the authors systematically explored the pH sensitivity of the Ber@ZnO-Z nanoplatform. The schematic diagram of the pH-responsive release mechanism of Ber@ZnO-Z (Fig. 9A) and the SEM images (Fig. 9B) manifested that when it was placed in an acidic environment, the shell ZIF-8 gradually collapsed, exposing the ZnO NSs and releasing the sterilization agent Ber. Whereafter, the ZnO NSs were further completely dissolved or transformed into smaller ZnO NPs, which lowered the pH of the solution. Moreover, the UV-visible (UV-vis) spectra (Fig. 9C) proved the characteristic peaks of ZnO NSs, ZnO-Z as well as Ber@ZnO-Z. The result pointed out the difference that Ber@ZnO-Z could decompose carriers with the addition of HCl, and the characteristic absorption band of Ber appeared, which was caused by the strong UV absorption capacity of ZnO, indicating that Ber@ZnO-Z with pH response characteristics could be used as a controlled release carrier to transfer active ingredients. Based on the principle, the pH-triggered Ber release behavior was explored, when the system was exposed to PBS buffer (pH 5.0, 6.5 and 8.0) at different times (Fig. 9D). The results signified that the structure of the ZIF-8 shell was destroyed under the action of acid, resulting in the release of Ber, whose release rate was highly pH-dependent, thereby achieving pH-triggered controlled release of the fungicide. Similarly, Ber@ZnO-Z also exhibited pH-responsive release behavior in acidic soil (Fig. 9E).

3.2 Enzyme-triggered therapy

Enzymes, a class of protein-structured biocatalysts that are ubiquitous in living organisms, regulate many biological processes.[155,156] When the body undergoes changes including enzyme deficiency, activity reduction or overexpression, abnormal catalytic reactions are often induced, which in turn lead to the occurrence and development of metabolic disorders and even diseases. Therefore, enzymes can be used as markers for disease detection and treatment, because of their high selectivity and specificity, which are also important internal stimuli for constructing responsive therapeutic systems. In view of this, researchers proposed to develop a pH/enzyme-responsive drug delivery system based on porous silica nanospheres

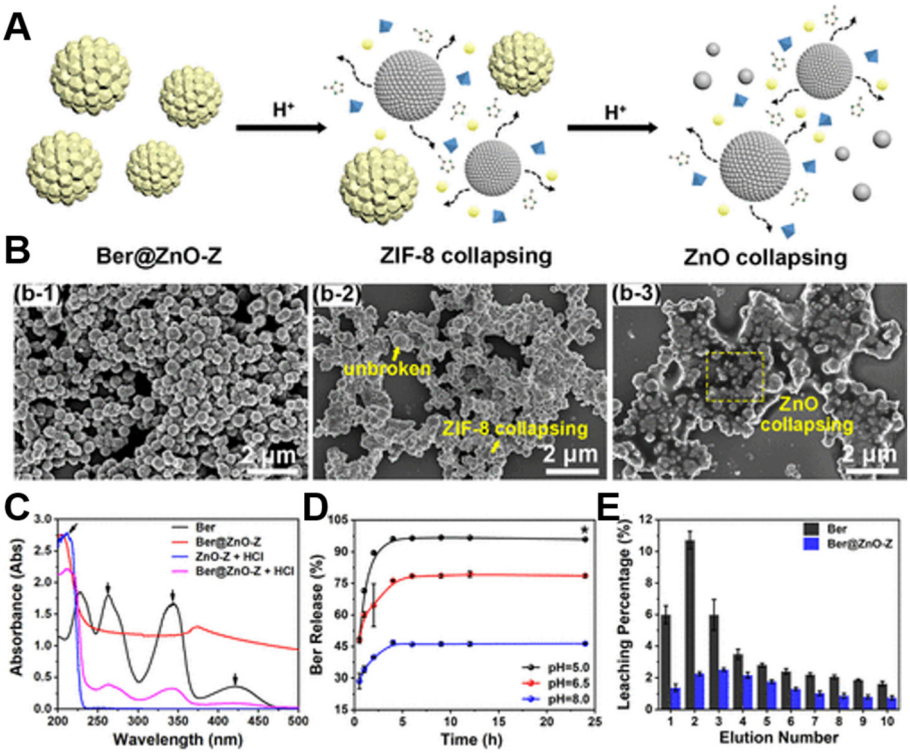

Fig. 9 (A) pH-responsive release mechanism of Ber@ZnO-Z. (B) SEM images of Ber@ZnO-Z at different pH values (8.0/6.5/5.0). (C) UV-vis spectroscopic analysis. (D) Cumulative release of Ber from Ber@ZnO-Z in PBS buffer at pH 5.0, 6.5 or 8.0. (E) Release of Ber and Ber@ZnO-Z in acidic soil. Adapted with permission from ref. 153, copyright 2022, American Chemical Society.

($pSiO_2$ NSs) and ZnO QDs, namely ZnO/HA gated $pSiO_2$/PCA-Glu NSs, in which ZnO QDs and hyaluronic acid (HA) acted as pH/enzyme-responsive gatekeepers for drug release, respectively.[157] Notably, HA could be particularly degraded by hyaluronidase (Hyal-1) overexpressed in the tumor microenvironment, which was beneficial to reduce premature drug release. Furthermore, Lai *et al.*[158] employed a multi-stage enzyme-responsive drug delivery program to design ZnO NPs hydrogel sheets that could efficiently treat corneal abrasion. The constructed functional nanocarriers were classified into three types according to their degradation responses to intraocular enzymes, including rapidly degrading dipalmitoyl phosphatidylcholine liposomes (DPPC), moderately degrading (low cross-linking) and slowly degrading (highly cross-linked) HA nanocarriers. Subsequently, a rabbit corneal abrasion model was built to verify the therapeutic effect of the hydrogel sheet, which suggested that the system could release the corresponding drugs (epigallocatechin gallate, β-1,3-glucan and SB431542) in three stages, achieving many functions such as early anti-inflammatory, mid-stage healing and late prevention of scar formation. All in all, the therapeutic hydrogel material could accommodate a variety of drug molecules, opening up a new avenue for the treatment of complex ocular diseases. Another study found that the designed porous ZnO–Co_3O_4 nanocages had inherent peroxidase-like activity, which could rapidly and specifically detect amyloid-β peptide, one of the main markers of early onset of Alzheimer's disease (AD).[159]

3.3 Other endogenous signals-triggered therapy

In addition to the above findings, the endogenous signaling molecule hydrogen sulfide (H_2S) is a key mediator of various physiological functions and pathological processes.[160] For instance, the excessive H_2S produced by colorectal cancer becomes a high potential target for disease treatment,[161] favoring the construction of endogenous gas signal activation nanoplatform. As is known to all, ZnO NPs are gas-sensing materials that have attracted much attention, and new gas sensors derived from them can be used for *in vitro* real-time detection of dangerous gases such as H_2S[162] and ammonia,[163] with low cost, weak toxicity, good responsiveness as well as easy structure control. In theory, ZnO NPs can also specifically respond to these endogenous gas signals, testifying promising potential in disease diagnosis and treatment.[164] Recent work by Zhou's group[165] validated this point, developing an oral bite pad based on the photoluminescent properties of ZnO QDs, which offered a method for accurately locating obvious and hidden dental lesions by detecting the local release of volatile sulfide. Herein, a ZnO-polydimethylsiloxane composite (ZnO-PDMS) was used to fabricate wearable fluorescent dental braces, which specifically responded to sulfides (mainly H_2S), resulting in fluorescence quenching, thereby realizing the visual and precise positioning of the patient's dental lesions and achieving the purpose of diagnosing the lesions (Fig. 10A and B). Additionally, Zhou *et al.*[166] reported an H_2S-responsive nanoplatform based on ZnO-coated virus-like silica (VZnO) nanoparticles, which reduced intracellular glutathione levels by reducing H_2S concentration, further contributing to ferroptosis in colorectal cancer cells and enabling efficient treatment of colorectal cancer (Fig. 10C).

Likewise, exosomal concentrations and exosome proteins are considered promising cancer biomarkers.[167,168] Qu *et al.*[169] synthesized a high surface area and strong affinity bayberry-like magnetic beads around ZnO nanowires for capturing exosomes. The authors successfully designed a fluorescence detection method for the simultaneous detection of exosome concentration and cancer-related exosomal proteins, possessing the characteristics of high sensitivity, low detection limit and good accuracy, which provided important reference value for the development of new biosensors for exosome analysis and intelligent disease diagnosis. In addition, the chemical

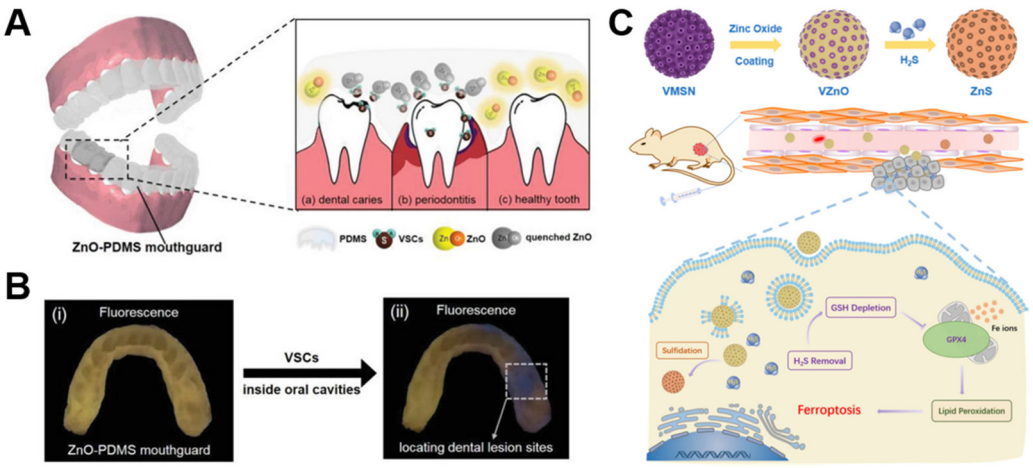

Fig. 10 (A) Schematic illustration of the ZnO-PDMS mouthguard and its response to sulfide, resulting from (a) caries, (b) periodontitis, and (c) healthy teeth. (B) Fluorescence images of the ZnO-PDMS mouthguard used to observe dental lesions *in vivo*: (i) before and (ii) after wearing by carious patients, to locate the lesions. Adapted with permission from ref. 165, copyright 2020, Wiley. (C) A schematic diagram of VZnO synthesis routes and H_2S removal for colorectal cancer treatment. Adapted with permission from ref. 166, copyright 2021, Springer.

gradient generated by the lesion can act as a driving force for self-driven reactive substances. Some researchers chose ZnO nanorods and sulfonated polystyrene microspheres to design an artificial swarm intelligence based on ion exchange reaction, which could be transmitted by the interaction between active particles to achieve long-range collective migration and aggregation under local gradient excitation.[170] Given their maneuverability and microscopic size, these artificial active material nanorobots were expected to be applied in biomedicine.[171]

4. Design and biomedical applications of multiple stimuli-responsive ZnO-based materials

Compared with single stimulus responsive materials, multi-stimuli-responsive materials have continued to be developed due to their versatility, and the corresponding multi-response synergistic therapy has yielded encouraging results.[172,173] As mentioned above, Wu *et al.*[74] reported DFT-C/ZnO-hydrogels that could simultaneously respond to light sources at two wavelengths (660 nm and 808 nm). The system played a photocatalytic antibacterial role under 660 nm red light irradiation and switched to a photothermal sterilization function under 808 nm NIR stimulation, which provided a strong guarantee for the healing of infected wounds. What's more, some researchers combined light and ultrasound as a stimulus source, and found that ZnO nanorods' light/piezoelectric double catalytic effect is higher than a single catalytic effect.[174] This was mainly attributed to the fact that the piezoelectric potential formed during the piezoelectric process helped to separate the photogenerated electron–hole pairs, thereby achieving a synergistic effect of photocatalysis and piezoelectric catalysis. In another study, Huo *et al.*[175] confirmed that cobalt (Co) foil modified with a new ZIF-67/ZnO hybrid coating achieved photoelectrocatalytic sterilization after exposure to visible light and potential stimulation.

In addition to combining the two extrinsic stimulus responsive strategies as described above, researchers have also attempted to combine the exogenous stimulus responsive strategy with the endogenous stimulus responsive strategy, thus achieving satisfactory results. For example, endogenous stimulation pH and exogenous stimulation light are simultaneously used as triggering mechanisms to construct a multifunctional dual stimulation responsive system for drug delivery, tumor treatment and wound healing.[176,177] Among them, Hahn *et al.*[136] incorporated acid-sensitive ZnO NPs into liposomes and loaded daunorubicin to construct a dual-responsive system of UV combined with pH, realizing the chemical photodynamic anticancer effect under the mode of acid-controlled drug release. Furthermore, Yang *et al.*[178] put forward a pH-responsive nanoplatform for 808 nm NIR mediated photodynamic therapy combined with chemotherapy, namely the α-$NaYbF_4$:Tm@CaF_2:Nd@ZnO-PAA-DOX nanoplatform. On the one hand, the polyacrylic acid (PAA) coating could cause its own disintegration in response to acidity, which in turn led to the efficient release of the loaded drug DOX at the tumor site. On the other hand, upconverting nanoparticles converted 808 nm NIR to UV (349 and 363 nm), excited the emergence of hole–electron pairs in ZnO, and then generated enough $^{\bullet}OH$ to kill tumor cells, while reducing the dependence on oxygen. It was worth mentioning that pH-triggered photothermal therapy systems also displayed excellent antitumor efficacy, such as the ZnO@polydopamine nanocomposites (ZnO@PDA-DOX/DNAzymes) designed by Zhou *et al.*[66] for chemical/gene/photothermal therapy. Similarly, the multi-mode combined treatment strategy of pH-responsive drug release combined with photodynamic/photothermal therapy based on ZnO-based nanomaterials is also suitable for the treatment of infected wounds, which solves the problems of poor treatment effect on wound healing by traditional single treatment methods.[179,180]

The multiple stimuli-responsive system centered on ZnO-based nanomaterials provides the possibility for targeted, on-demand, precise and efficient treatment of diseases, revealing broad application prospects in the field of biomedicine (Table 4). The continuous development of the multi-response collaborative treatment platform can not only reduce the excessive dependence on a single stimulus, but also increase the sensitivity and compliance of the platform when treating different patients.[181,182] Although the multi-responsive strategy developed around ZnO has made gratifying achievements,

Table 4 Representative biomedical applications of ZnO-based nanomaterials with multiple responsive systems

Nanoplatform	Responsive strategy	Application field	Findings	Ref.
UZNP-PAA-DOX	808 nm NIR and pH	Antitumor	The system realized the targeted delivery of drugs and multi-strategy anti-tumor effect	178
ZnO@PDA	808 nm NIR and pH	Antitumor	Chemical/gene/PTT had a highly effective anti-tumor effect	66
Ti-ZnO@Col-I	583 nm yellow light and 808 nm NIR	Peri-implant diseases	Dual light-responsive coatings provided customized treatments for peri-implantitis	56
PDA-rGO-ZnO	Electricity and 583 nm yellow light	Wound healing	Photoelectric dual stimulation accelerated wound repair	57
Ag/Ag@AgCl/ZnO	Visible light and pH	Wound healing	This hybrid system could boost the immune system and speed wound healing	179
ZnO QDs@GO-CS	808 nm NIR and pH	Wound healing	The platform combined photothermal and chemokinetic effects for antibacterial and pro-healing functions	180

there are still some problems to be solved in future development and application. First of all, the current multi-stimuli responsive ZnO-based materials combine different strategies, and the explanation of the basic mechanism of complementary and synergistic effects of specific strategies is missing, which should be fully considered in future work. Secondly, ZnO-based biomaterials generally contain a variety of components and complex structures, as well as the related manufacturing processes are cumbersome and need to be further facilitated. Finally, the existing multi-stimuli responsive ZnO system is still focused on basic research, and its clinical transformation remains to be realized.

5. Conclusion and outlook

This paper systematically summarizes the classification of ZnO nanomaterial based intelligent responsive systems in recent years, and reviews the application of related stimulus responsive systems in the biomedical field. Compared with single ZnO-based biomaterials, the application of stimuli-responsive systems has incomparable advantages, including safety, efficiency, maneuverability and multi-functionality, which makes it possible to formulate personalized treatment strategies.

Stimuli-responsive materials are a class of materials that convert external stimuli into changes in their own dynamic structures or shapes through multiple approaches, thereby obtaining other peculiar physicochemical properties. According to the source of stimulation, stimuli-responsive ZnO-based materials can be divided into two categories, namely, responding to exogenous stimuli (light, ultrasound, mechanical force, *etc.*) and endogenous stimuli (pH, enzymes, gas signal molecules, *etc.*) of smart materials. Here, we first focus on the basic structure, response characteristics and application advantages of ZnO-based materials responsive to exogenous stimuli such as light, ultrasound and mechanical force. Related responsive systems have been commonly used in various aspects of the biomedical field. Second, the construction of endogenous stimulus responsive systems about ZnO-based nanomaterials is discussed. Endogenous response ZnO-based materials can respond to endogenous signals related to the presence or high degree of imbalance in the lesion location, including pH, enzymes, H_2S gas signaling molecules, *etc.*, further achieving active on-demand administration and efficient and accurate treatment, thus effectively reducing the impact of additional human intervention. In addition, a multi-stimuli-responsive ZnO-based biomaterial system can be designed to integrate various responsive materials on demand to flexibly implement various required diagnostic and therapeutic functions. Stimuli-responsive ZnO-based nanomaterials are widely utilized in the field of biomedicine, and play a role in improving the defects of existing therapies and the curative effect in drug delivery, disease diagnosis and disease treatment, showing potential to realize intelligent and personalized medicine.

Notably, the development and clinical application of stimuli-responsive ZnO-based biomaterials are still challenging. First, the commonly used preparations in multiple stimulus responsive systems are mainly multi-component materials, which have problems such as complex synthesis procedures and poor stability of synthetic materials. Moreover, multiple stimulus responsive systems often involve multiple stimulus sources, increasing the difficulty of operation. Most importantly, the long-term biocompatibility and *in vivo* metabolism of existing ZnO NP formulations are unclear, which limits further applications of the material. In future research, the physicochemical properties of ZnO NPs can be further optimized based on these contents, and a more practical, more stable, more convenient, safer and simpler stimulus-responsive system can be constructed. At present, such a multi-functional intelligent responsive therapy system is still in the laboratory research stage, and it also faces huge challenges on the way out of the laboratory into clinical practice. The construction of a multi-functional intelligent response platform based on ZnO is inseparable from the research and communication of multidisciplinary staff, which is also conducive to the clinical application of stimulus response system.

Conflicts of interest

There are no conflicts to declare.

Acknowledgements

This work was funded by the National Natural Science Foundation of China (No. 31860263 to Xiaolei Wang), the Key Youth Project of Jiangxi Province (20202ACB216002 to Xiaolei Wang), the Key Research and Development Project of Jiangxi Province (20212BBG73004 to Xiaolei Wang), and the Graduate Innovation Special Fund Project of Jiangxi Province (YC2022-B005 to Zhenzhen Weng).

References

1 G. Schmidl, G. Jia, A. Gawlik, G. Andrä, K. Richter and J. Plentz, *Mater. Today Energy*, 2021, **21**, 100811.
2 J. Xu, H. He, X. Jian, K. Qu, J. Xu, C. Li, Z. Gao and Y. Song, *Anal. Chem.*, 2021, **93**, 9286–9295.
3 F. Fu, D. Yang, H. Wang, Y. Qian, F. Yuan, J. Zhong and X. Qiu, *ACS Sustainable Chem. Eng.*, 2019, **7**, 16419–16427.
4 M. Zabilskiy, V. Sushkevich, M. A. Newton, F. Krumeich, M. Nachtegaal and J. A. V. Bokhoven, *Angew. Chem., Int. Ed.*, 2021, **60**, 17053–17059.
5 J. A. Ruszkiewicz, A. Pinkas, B. Ferrer, T. V. Peres, A. Tsatsakis and M. Aschner, *Toxicol. Rep.*, 2017, **4**, 245–259.

6 C. Hanley, J. Layne, A. Punnoose, K. Reddy, I. Coombs, A. Coombs, K. Feris and D. Wingett, *Nanotechnology*, 2008, **19**, 295103.
7 X. Wu, S. Liu, H. Zhu, Z. Ma, X. Dai and W. Liu, *Adv. Sci.*, 2022, **9**, 2103982.
8 Y. Deng, C. Yang, Y. Zhu, W. Liu, H. Li, L. Wang, W. Chen, Z. Wang and L. Wang, *Nano Lett.*, 2022, **22**, 2702–2711.
9 P. Sadhukhan, M. Kundu, S. Chatterjee, N. Ghosh, P. Manna, J. Das and P. C. Sil, *Mater. Sci. Eng., C*, 2019, **100**, 129–140.
10 P. Sathishkumar, Z. Li, R. Govindan, R. Jayakumar, C. Wang and F. Gu, *Appl. Surf. Sci.*, 2021, **536**, 147741.
11 H. Hong, J. Shi, Y. Yang, Y. Zhang, J. Engle, R. Nickles, X. Wang and W. Cai, *Nano Lett.*, 2011, **11**, 3744–3750.
12 K. Vimala and K. Soundarapandian, *Ann. Oncol.*, 2016, **27**, ix38–ix39.
13 A. Khan, K. Huang, M. Khalaji, F. Yu, X. Xie, T. Zhu, Y. Morsi, J. Zhao and X. Mo, *Bioact. Mater.*, 2021, **6**, 2783–2800.
14 F. Deng, Z. Bu, H. Hu, X. Huang, Z. Liu and C. Ning, *Appl. Mater. Today*, 2022, **27**, 101433.
15 X. Wang, M. Shan, S. Zhang, X. Chen, W. Liu, J. Chen and X. Liu, *Adv. Sci.*, 2022, **9**, 2104843.
16 S. S. Said, S. Campbell and T. Hoare, *Chem. Mater.*, 2019, **31**, 4971–4989.
17 P. Lavrador, M. Esteves, V. Gaspar and J. Mano, *Adv. Funct. Mater.*, 2021, **31**, 2005941.
18 Z. Fu, L. Ouyang, R. Xu, Y. Yang and W. Sun, *Mater. Today*, 2022, **52**, 112–132.
19 B. Ortiz-Casas, A. Galdámez-Martínez, J. Gutiérrez-Flores, A. Ibañez, P. Panda, G. Santana, H. A. D. L. Vega, M. Suar, C. Rodelo, A. Kaushik, Y. Mishra and A. Dutt, *Mater. Today*, 2021, **50**, 533–569.
20 H. Fatima, Z. Jin, Z. Shao and X. Chen, *J. Colloid Interface Sci.*, 2022, **621**, 440–463.
21 D. Wang, X. Yang, H. Yu, J. Gu, D. Qi, J. Yao and Q. Ni, *J. Hazard. Mater.*, 2020, **383**, 121123.
22 S. Chen, Z. Huang, M. Yuan, G. Huang, H. Guo, G. Meng, Z. Feng and P. Zhang, *J. Mater. Sci. Technol.*, 2022, **125**, 67–80.
23 Y. Li, Y. Li, Y. Bai, R. Wang, L. Lin and Y. Sun, *RSC Adv.*, 2020, **10**, 38416–38423.
24 P. Sivakumar, M. Lee, Y. Kim and M. Shim, *J. Mater. Chem. B*, 2018, **6**, 4852–4871.
25 N. Chauhan, S. Gupta, D. Avasthi, R. Adelung, Y. Mishra and U. Jain, *ACS Appl. Mater. Interfaces*, 2018, **10**, 30631–30639.
26 X. Miao, F. Yu, K. Liu, Z. Lv, J. Deng, T. Wu, X. Cheng, W. Zhang, X. Cheng and X. Wang, *Bioact. Mater.*, 2022, **7**, 181–191.
27 S. Cao, Y. Xia, J. Shao, B. Guo, Y. Dong, I. Pijpers, Z. Zhong, F. Meng, L. K. E. A. Abdelmohsen, D. Williams and J. Hest, *Angew. Chem., Int. Ed.*, 2021, **60**, 17629–17637.
28 C. Chu, J. Yu, E. Ren, S. Ou, Y. Zhang, Y. Wu, H. Wu, Y. Zhang, J. Zhu, Q. Dai, X. Wang, Q. Zhao, W. Li, Z. Liu, X. Chen and G. Liu, *Adv. Sci.*, 2020, **7**, 2000346.
29 X. Ge, H. Cui, J. Kong, S. Lu, R. Zhan, J. Gao, Y. Xu, S. Lin, K. Meng, L. Zu, S. Guo and L. Zheng, *Adv. Mater.*, 2020, **32**, 2000037.
30 M. Zhu, H. Zhang, G. Ran, Y. Yao, Z. Yang, Y. Ning, Y. Yu, R. Zhang, X. Peng, J. Wu, Z. Jiang, W. Zhang, B. Wang, S. Gao and J. Zhang, *Angew. Chem., Int. Ed.*, 2022, **61**, e202204330.
31 H. P. Lee and A. K. Gaharwar, *Adv. Sci.*, 2020, **7**, 2000863.
32 Z. Youssef, R. Vanderesse, L. Colombeau, F. Baros, T. Roques-Carmes, C. Frochot, H. Wahab, J. Toufaily, T. Hamieh, S. Acherar and A. Gazzali, *Cancer Nanotechnol.*, 2017, **8**, 1–62.
33 S. Hackenberg, A. Scherzed, M. Kessler, K. Froelich, C. Ginzkey, C. Koehler, M. Burghartz, R. Hagen and N. Kleinsasser, *Int. J. Oncol.*, 2010, **37**, 1583–1590.
34 S. Noimark, J. Weiner, N. Noor, E. Allan, C. Williams, M. Shaffer and I. Parkin, *Adv. Funct. Mater.*, 2015, **25**, 1367–1373.
35 A. Ancona, B. Dumontel, N. Garino, B. Demarco, D. Chatzitheodoridou, W. Fazzini, H. Engelke and V. Cauda, *Nanomaterials*, 2018, **8**, 143.
36 X. Wang, S. Xu, E. Chalmers, X. Chen, Y. Liu and X. Liu, *ACS Appl. Mater. Interfaces*, 2022, **14**, 10769–10781.
37 A. Holmes, Z. Song, H. Moghimi and M. Roberts, *ACS Nano*, 2016, **10**, 1810–1819.
38 A. Ginzburg, R. S. Blackburn, C. Santillan, L. Truong, R. Tanguay and J. Hutchison, *Photochem. Photobiol. Sci.*, 2021, **20**, 1273–1285.
39 M. Kciuk, B. Marciniak, M. Mojzych and R. Kontek, *Int. J. Mol. Sci.*, 2020, **21**, 7264.
40 L. Siebert, E. Luna-Cerón, L. García-River, J. S. Oh, J. Jang, D. Rosas-Gómez, M. Pérez-Gómez, G. Maschkowitz, H. Fickenscher, D. Oceguera-Cuevas, C. Holguín-León, B. Byambaa, M. Hussain, E. Enciso-Martínez, M. Cho, Y. Lee, N. Sobahi, A. Hasan, D. Orgill, Y. Mishr, R. Adelung, E. Lee and S. Shin, *Adv. Funct. Mater.*, 2021, **31**, 2007555.
41 C. Shuai, X. Yuan, Y. Shuai, G. Qian, J. Yao, W. Xu, S. Peng and W. Yang, *Mater. Today Nano*, 2022, **18**, 100210.
42 H. Fu, Z. Feng, S. Liu, P. Wang, C. Zhao and C. Wang, *Chin. Chem. Lett.*, 2022, DOI: **10.1016/j.cclet.2022.04.023**.
43 X. Guo, J. Duan, W. Wang and Z. Zhang, *Fuel*, 2020, **280**, 118544.
44 Y. Dong, Z. Liu, Y. Ning, S. Armes and D. Li, *Chem. Mater.*, 2022, **34**, 3357–3364.
45 W. Jiang, J. Low, K. Mao, D. Duan, S. Chen, W. Liu, C. Pao, J. Ma, S. Sang, C. Shu, X. Zhan, Z. Qi, H. Zhang, Z. Liu, X. Wu, R. Long, L. Song and Y. Xiong, *J. Am. Chem. Soc.*, 2021, **143**, 269–278.
46 M. Rani, J. Yadav, K. Shu and U. Shanker, *J. Colloid Interface Sci.*, 2021, **601**, 689–703.
47 Y. Zhao, L. Xu, L. Tan, D. Li and R. Qiao, *Mater. Lett.*, 2021, **293**, 129719.
48 Y. Jiang, Z. Xiong, J. Huang, F. Yan, G. Yao and B. Lai, *Chin. Chem. Lett.*, 2022, **33**, 415–423.

49 P. Sánchez-Cid, C. Jaramillo-Páez, J. A. Navío, A. N. Martín-Gómez and M. C. Hidalgo, *J. Photochem. Photobiol., A*, 2019, **369**, 119–132.
50 S. Ansari, M. Khan, S. Kalathil, A. Nisar, J. Lee and M. Cho, *Nanoscale*, 2013, **5**, 9238–9246.
51 M. Arakha, J. Roy, P. S. Nayak, B. Mallick and S. Jha, *Free Radicals Biol. Med.*, 2017, **110**, 42–53.
52 L. Sun, Y. Guo, Y. Hu, S. Pan and Z. Jiao, *Sens. Actuators, B*, 2021, **337**, 129793.
53 X. Yu, H. Chen, Q. Ji, Y. Chen, Y. Wei, N. Zhao and B. Yao, *Chemosphere*, 2021, **267**, 129285.
54 C. Zhang, Y. Yi, H. Yang, Z. Yi, X. Chen, Z. Zhou, Y. Yi, H. Li, J. Chen and C. Liu, *Appl. Mater. Today*, 2022, **28**, 101531.
55 J. Gupta and D. Bahadur, *ACS Sustainable Chem. Eng.*, 2017, **5**, 8702–8709.
56 S. Zhao, Y. Xu, W. Xu, Z. Weng, F. Cao, X. Wan, T. Cui, Y. Yu, L. Liao and X. Wang, *ACS Appl. Mater. Interfaces*, 2020, **12**, 30044–30051.
57 Z. Weng, F. Yu, Q. Leng, S. Zhao, Y. Xu, W. Zhang, Z. Zhu, J. Ye, Q. Wei and X. Wang, *Mater. Sci. Eng., C*, 2021, **124**, 112066.
58 S. Zhao, X. Yang, Y. Xu, Z. Weng, L. Liao and X. Wang, *Nano Res.*, 2022, **15**, 5245–5255.
59 H. Cheng, H. Liu, Z. Liu, Z. Xu, X. Liu, S. Jia, C. He, S. Liu, J. Zhang and X. Wang, *Nano Res.*, 2022, **15**, 6297–6305.
60 Y. Sun, W. Zhang, M. Wang, H. Liu, Q. Li, J. Luo, M. Zhao, S. Liu and X. Wang, *Nano Res.*, 2022, DOI: **10.1007/s12274-022-4744-1**.
61 B. Huang, X. Liu, Z. Li, Y. Zheng, K. W. K. Yeung, Z. Cui, Y. Liang, S. Zhu and S. Wu, *Chem. Eng. J.*, 2021, **414**, 128805.
62 H. Yang, Q. Zhang, Y. Chen, Y. Huang, F. Yang and Z. Lu, *Carbohydr. Polym.*, 2018, **201**, 162–171.
63 N. Yu, H. Peng, L. Qiu, R. Wang, C. Jiang, T. Cai, Y. Sun, Y. Li and H. Xiong, *Int. J. Biol. Macromol.*, 2019, **141**, 207–217.
64 S. Zhang, Y. Li, Z. Li, G. Wang, A. Liao, J. Wang, H. Li, Z. Gu, B. Y. Cheng and X. Zhang, *Small*, 2022, **18**, 2200038.
65 M. Zhang, W. Wang, M. Mohammadniaei, T. Zheng, Q. Zhang, J. Ashley, S. Liu, Y. Sun and B. Tang, *Adv. Mater.*, 2021, **33**, 2008802.
66 M. Liu, Y. Peng, Y. Nie, P. Liu, S. Hu, J. Ding and W. Zhou, *Acta Biomater.*, 2020, **110**, 242–253.
67 K. Vimala, K. Shanthi, S. Sundarraj and S. Kannan, *J. Colloid Interface Sci.*, 2017, **488**, 92–108.
68 X. Fan, F. Yang, J. Huang, Y. Yang, C. Nie, W. Zhao, L. Ma, C. Cheng, C. Zhao and R. Haag, *Nano Lett.*, 2019, **19**, 5885–5896.
69 J. Fang, Y. Wan, Y. Sun, X. Sun, M. Qi, S. Cheng, C. Li, Y. Zhou, L. Xu, B. Dong and L. Wang, *Chem. Eng. J.*, 2022, **435**, 134935.
70 J. Zou, Z. Yin, P. Wang, D. Chen, J. Shao, Q. Zhang, L. Sun, W. Huang and X. Dong, *Chem. Sci.*, 2018, **9**, 2188–2194.
71 C. Mao, Y. Xiang, X. Liu, Y. Zheng, K. Yeung, Z. Cui, X. Yang, Z. Li, Y. Liang, S. Zhu and S. Wu, *ACS Appl. Mater. Interfaces*, 2019, **11**, 17902–17914.
72 Q. Lei, D. He, L. Ding, F. Kong, P. He, J. Huang, J. Guo, C. J. Brinker, G. Luo, W. Zhu and Y. Yu, *Adv. Funct. Mater.*, 2022, **32**, 2113269.
73 J. Li, X. Liu, L. Tan, Y. Liang, Z. Cui, X. Yang, S. Zhu, Z. Li, Y. Zheng, K. Yeung, X. Wang and S. Wu, *Small Methods*, 2019, **3**, 1900048.
74 Y. Xiang, C. Mao, X. Liu, Z. Cui, D. Jing, X. Yang, Y. Liang, Z. Li, S. Zhu, Y. Zheng, K. Yeung, D. Zheng, X. Wang and S. Wu, *Small*, 2019, **15**, 1900322.
75 Q. Yao, J. Fan, S. Long, X. Zhao, H. Li, J. Du, K. Shao and X. Peng, *Chem*, 2022, **8**, 197–209.
76 W. Chen, C. He, N. Qiao, Z. Guo, S. Hu, Y. Song, H. Wang, Z. Zhang, B. Ke and X. Sun, *Biomaterials*, 2022, **286**, 121582.
77 W. Xiu, L. Wan, K. Yang, X. Li, L. Yuwen, H. Dong, Y. Mou, D. Yang and L. Wang, *Nat. Commun.*, 2022, **13**, 3875.
78 W. Huang, F. Wang, A. Shen, L. Zhang, X. Nie, Z. Zhang, G. Chen, L. Xia, L. Wang, S. Ding, Q. Meng, W. Zhang, C. Hong and Y. You, *Mater. Horiz.*, 2021, **8**, 645–645.
79 F. Dong, Q. Jiang, L. Li, T. Liu, S. Zuo, L. Gao, M. Fang, Y. Gao, B. Sun, C. Luo, Z. He and J. Sun, *Nano Res.*, 2022, **15**, 3422–3433.
80 Y. Chen, M. Du, Z. Yuan, Z. Chen and F. Yan, *Nat. Commun.*, 2022, **13**, 4468.
81 H. Jiang, N. M. Carter, A. Zareei, S. Nejati, J. Waimin, S. Chittiboyina, E. Niedert, T. Soleimani, S. Lelièvre, C. Goergen and R. Rahim, *ACS Appl. Bio Mater.*, 2020, **3**, 4012–4024.
82 K. Bian, W. Yang, Y. Xu, W. Zeng, H. Wang, H. Liang, T. Cui, Z. Wang and B. Zhang, *Small*, 2022, **18**, 2202921.
83 X. Wang, M. Wu, H. Li, J. Jiang, S. Zhou, W. Chen, C. Xie, X. Zhen and X. Jiang, *Adv. Sci.*, 2022, **9**, 2104125.
84 G. Wang, C. Zhang, Y. Jiang, Y. Song, J. Chen, Y. Sun, Q. Li, Z. Zhou, Y. Shen and P. Huang, *Adv. Funct. Mater.*, 2021, **31**, 202102786.
85 A. Athanassiadis, Z. Ma, N. Moreno-Gomez, K. Melde, E. Choi, R. Goyal and P. Fischer, *Chem. Rev.*, 2022, **122**, 5165–5208.
86 Z. Cao, G. Yuan, L. Zeng, L. Bai, X. Liu, M. Wu, R. Sun, Z. Chen, Y. Jiang, Q. Gao, Y. Chen, Y. Zhang, Y. Pan and J. Wang, *ACS Nano*, 2022, **16**, 10608–10622.
87 D. Wu, J. Li, S. Xu, Q. Xie, Y. Pan, X. Liu, R. Ma, H. Zheng, M. Gao, W. Wang, J. Li, X. Cai, F. Jaouen and R. Li, *J. Am. Chem. Soc.*, 2020, **142**, 19602–19610.
88 S. Shaikh, M. Younis, F. Rehman, H. Jiang and X. Wang, *Langmuir*, 2020, **36**, 9472–9480.
89 W. Chen, C. Liu, X. Ji, J. Joseph, Z. Tang, J. Ouyang, Y. Xiao, N. Kong, N. Joshi, O. Farokhzad, W. Tao and T. Xie, *Angew. Chem., Int. Ed.*, 2022, **440**, 135812.
90 C. Lops, A. Ancona, K. D. Cesare, B. Dumontel, N. Garino, G. Canavese, S. Hérnandez and V. Cauda, *Appl. Catal., B*, 2019, **243**, 629–640.

91 R. Mahdavi and S. Talesh, *Ultrason. Sonochem.*, 2019, **51**, 230–240.
92 X. Wang, X. Zhong, L. Bai, J. Xu, F. Gong, Z. Dong, Z. Yang, Z. Zeng, Z. Liu and L. Cheng, *J. Am. Chem. Soc.*, 2020, **142**, 6527–6537.
93 Y. Xu, S. Zhao, Z. Weng, W. Zhang, X. Wan, T. Cui, J. Ye, L. Liao and X. Wang, *ACS Appl. Mater. Interfaces*, 2020, **12**, 54497–54506.
94 J. Sei and T. J. Webster, *Nanotechnology*, 2012, **23**, 495101.
95 K. Barick, S. Nigam and D. Bahadur, *J. Mater. Chem.*, 2010, **20**, 6446–6452.
96 B. Geng, S. Xu, P. Li, X. Li, F. Fang, D. Pan and L. Shen, *Small*, 2022, **18**, 2103528.
97 X. Pan, N. Wu, S. Tian, J. Guo, C. Wang, Y. Sun, Z. Huang, F. Chen, Q. Wu, Y. Jing, Z. Yin, B. Zhao, X. Xiong, H. Liu and D. Zhou, *Adv. Funct. Mater.*, 2022, **32**, 2112145.
98 P. Gholami, L. Dinpazhoh, A. Khataee and Y. Orooji, *Ultrason. Sonochem.*, 2019, **55**, 44–56.
99 D. Xiang, Z. Liu, M. Wu, H. Liu, X. Zhang, Z. Wang, Z. Wang and L. Li, *Small*, 2020, **16**, 1907603.
100 Y. Liu, Y. Wang, W. Zhen, Y. Wang, S. Zhang, Y. Zhao, S. Song, Z. Wu and H. Zhang, *Biomaterials*, 2020, **251**, 120075.
101 Q. Hoang, V. Ravichandran, T. Cao, J. Kang, Y. Ko, T. Lee and M. Shim, *Chem. Eng. J.*, 2022, **435**, 135039.
102 H. Fukui, R. Chow, J. Xie, Y. Foo, C. Yap, N. Minc, N. Mochizuki and J. Vermot, *Science*, 2021, **374**, 351–354.
103 J. Frith, G. Kusuma, J. Carthew, F. Li, N. Cloonan, G. Gomez and J. Cooper-White, *Nat. Commun.*, 2018, **9**, 257.
104 M. Wu, Z. Zhang, Z. Liu, J. Zhang, Y. Zhang, Y. Ding, T. Huang, D. Xiang, Z. Wang, Y. Dai, X. Wan, S. Wang, H. Qian, Q. Sun and L. Li, *Nano Today*, 2021, **37**, 101104.
105 N. Hao, Z. Xu, Y. Nie, C. Jin, A. Closson, M. Zhang and J. Zhang, *Chem. Eng. J.*, 2019, **378**, 122222.
106 T. Lee, D. Kim, M. E. Suk, G. Bang, J. Choi, J. Bae, J. Yoon, W. Moon and D. Choi, *Adv. Funct. Mater.*, 2021, **31**, 2104372.
107 J. Marmolejo-Tejada, J. Roche-Yepes, C. Pérez-López, J. Taborda, A. Ávila and A. Jaramillo-Botero, *J. Chem. Inf. Model.*, 2021, **61**, 4537–4543.
108 R. Augustine, P. Dan, A. Sosnik, N. Kalarikkal, N. Tran, B. Vincent, S. Thomas, P. Menu and D. Rouxel, *Nano Res.*, 2017, **10**, 3358–3376.
109 Z. Wang, J. Wang, J. Ayarza, T. Steeves, Z. Hu, S. Manna and A. Esser-Kahn, *Nat. Mater.*, 2021, **20**, 869–874.
110 O. Careta, J. Fornell, E. Pellicer, E. Ibañez, A. Blanquer, J. Esteve, J. Sort, G. Murillo and C. Nogués, *Biomedicines*, 2021, **9**, 352.
111 S. Bhang, W. Jang, J. Han, J. Yoon, W. La, E. Lee, Y. Kim, J. Shin, T. Lee, H. Baik and B. Kim, *Adv. Funct. Mater.*, 2017, **27**, 1603497.
112 J. Yoon, M. Misra, S. Yu, H. Kim, S. Bhang, S. Song, J. Lee, S. Ryu, Y. Choo, G. Jeong, S. Kwon, S. Im, T. Lee and B. Kim, *Adv. Funct. Mater.*, 2017, **27**, 1703853.
113 Y. Qian, Y. Cheng, J. Song, Y. Xu, W. Yuan, C. Fan and X. Zheng, *Small*, 2020, **16**, 2000796.
114 G. Murillo, A. Blanquer, C. Vargas-Estevez, L. Barrios, E. Ibáñez, C. Nogués and J. Esteve, *Adv. Mater.*, 2017, **29**, 1605048.
115 Y. Li, L. Sun and T. Webster, *J. Biomed. Nanotechnol.*, 2018, **14**, 536–545.
116 J. Liang, H. Zeng, L. Qiao, H. Jiang, Q. Ye, Z. Wang, B. Liu and Z. Fan, *ACS Appl. Mater. Interfaces*, 2022, **14**, 30507–30522.
117 E. Bratanis, T. Andersson, R. Lood and E. Bukowska-Faniband, *Front. Microbiol.*, 2020, **11**, 662.
118 Y. Tang, Q. Huang, D. Zheng, Y. Chen, L. Ma, C. Huang and X. Zhang, *Mater. Today*, 2022, **53**, 71–83.
119 N. Gogurla, B. Roy and S. Kim, *Nano Energy*, 2020, **77**, 105242.
120 Y. Tan, K. Yang, B. Wang, H. Li, L. Wang and C. Wang, *Nano Res.*, 2021, **14**, 3969–3976.
121 G. Lee, J. H. Son, S. Lee, S. Kim, D. Kim, N. Nguyen, S. Lee and K. Cho, *Adv. Sci.*, 2021, **8**, 2002606.
122 Y. Wang, H. Zhao, J. Cheng, B. Liu, Q. Fu and Y. Wang, *Nanomicro Lett.*, 2022, **14**, 76.
123 Y. Song, F. Yin, C. Zhang, W. Guo, L. Han and Y. Yuan, *Nanomicro Lett.*, 2021, **13**, 76.
124 H. Peng, B. Cui, G. Li, Y. Wang, N. Li, Z. Chang and Y. Wang, *Mater. Sci. Eng., C*, 2015, **46**, 253–263.
125 J. Wang, Z. Jia, X. Liu, J. Dou, B. Xu, B. Wang and G. Wu, *Nano-Micro Lett.*, 2021, **13**, 175.
126 H. Peng, C. Hu, J. Hu, X. Tian and T. Wu, *Microporous Mesoporous Mater.*, 2016, **226**, 140–145.
127 Z. Sun, C. Song, C. Wang, Y. Hu and J. Wu, *Mol. Pharm.*, 2020, **17**, 373–391.
128 M. Carofiglio, M. Laurenti, V. Vighetto, L. Racca, S. Barui, N. Garino, R. Gerbaldo, F. Laviano and V. Cauda, *Nanomaterials*, 2021, **11**, 2628.
129 A. B. Cook and P. Decuzzi, *ACS Nano*, 2021, **15**, 2068–2098.
130 H. Dai, T. Sun, T. Han, Z. Guo, X. Wang and Y. Chen, *Environ. Res.*, 2020, **191**, 110086.
131 J. Wang, C. Qu, X. Shao, G. Song, J. Sun, D. Shi, R. Jia, H. An and H. Wang, *Bioact. Mater.*, 2023, **20**, 404–417.
132 H. Yang, Y. Ding, Z. Tong, X. Qian, H. Xu, F. Lin, G. Sheng, L. Hong, W. Wang and Z. Mao, *Theranostics*, 2022, **12**, 4250–4268.
133 S. Zhang, J. Lv, P. Gao, Q. Feng, H. Wang and Y. Cheng, *Nano Lett.*, 2021, **21**, 7855–7861.
134 J. Liu, Y. Kang, S. Yin, A. Chen, J. Wu, H. Liang and L. Shao, *Small*, 2019, **15**, 1901073.
135 Q. Yuan, S. Hein and R. D. K. Misra, *Acta Biomater.*, 2010, **6**, 2732–2739.
136 N. Tripathy, R. Ahmad, H. Ko, G. Khang and Y. Hahn, *Nanoscale*, 2015, **7**, 4088–4096.
137 F. Muhammad, M. Guo, W. Qi, F. Sun, A. Wang, Y. Guo and G. Zhu, *J. Am. Chem. Soc.*, 2011, **133**, 8778–8781.
138 J. Zhang, D. Wu, M. Li and J. Feng, *ACS Appl. Mater. Interfaces*, 2015, **7**, 26666–26673.
139 X. Huang, S. Wu and X. Du, *Carbon*, 2016, **101**, 135–142.

140 X. Xiao, S. Liang, Y. Zhao, D. Huang, B. Xing, Z. Cheng and J. Lin, *Nanoscale*, 2020, **12**, 3846–3854.
141 R. Dhivya, M. Rajasekaran, J. Annaraj, J. Ranjani and J. Rajendhran, *Adv. Mater. Lett.*, 2015, **6**, 505–512.
142 M. Kundu, P. Sadhukhan, N. Ghosh, S. Chatterjee, P. Manna, J. Das and P. Sil, *J. Adv. Res.*, 2019, **18**, 161–172.
143 X. Cai, Y. Luo, W. Zhang, D. Du and Y. Lin, *ACS Appl. Mater. Interfaces*, 2016, **8**, 22442–22450.
144 D. Depan and R. Misra, *J. Biomed. Mater. Res.*, 2014, **102**, 2934–2941.
145 F. Muhammad, M. Guo, Y. Guo, W. Qi, F. Qu, F. Sun, H. Zhao and G. Zhu, *J. Mater. Chem.*, 2011, **21**, 13406–13412.
146 D. Ye, Y. Ma, W. Zhao, H. Cao, J. Kong, H. Xiong and H. Möhwald, *ACS Nano*, 2016, **10**, 4294–4300.
147 Y. Wang, S. Song, J. Liu, D. Liu and H. Zhang, *Angew. Chem., Int. Ed.*, 2015, **54**, 536–540.
148 X. Cai, Y. Luo, H. Yan, D. Du and Y. Lin, *ACS Appl. Mater. Interfaces*, 2017, **9**, 5739–5747.
149 X. Chen, T. Niu, Y. Gao, X. Liang, S. Li, L. Zhang, L. Li, T. Wang, Z. Su and C. Wang, *Chem. Eng. J.*, 2019, **371**, 443–451.
150 J. Wang, J. Lee, D. Kim and L. Zhu, *ACS Appl. Mater. Interfaces*, 2017, **9**, 39971–39984.
151 T. Cui, Z. Yan, H. Qin, Y. Sun, J. Ren and X. Qu, *Small*, 2019, **15**, 1903323.
152 J. Wang, S. Yu, Q. Wu, X. Gong, S. He, J. Shang, X. Liu and F. Wang, *Angew. Chem., Int. Ed.*, 2021, **60**, 10766–10774.
153 W. Liang, J. Cheng, J. Zhang, Q. Xiong, M. Jin and J. Zhao, *ACS Nano*, 2022, **16**, 2762–2773.
154 Y. Huang, Q. Gao, C. Li, X. Chen, X. Li, Y. He, Q. Jin and J. Ji, *Adv. Funct. Mater.*, 2022, **32**, 2109011.
155 P. Qiu, M. Huang, S. Wu, M. Wen, N. Yu and Z. Chen, *ACS Appl. Mater. Interfaces*, 2022, **14**, 29537–29549.
156 M. Yi, F. Wang, W. Tan, J. Hsieh, E. Egelman and B. Xu, *J. Am. Chem. Soc.*, 2022, **144**, 13055–13059.
157 L. Qiu, W. Zhang, S. Wang, X. Zhang, Y. Zhao, L. Cao and L. Sun, *Mater. Sci. Eng., C*, 2017, **81**, 485–491.
158 L. Luo, D. D. Nguyen, C. Huang and J. Lai, *Chem. Eng. J.*, 2022, **429**, 132409.
159 X. Zhou, S. Wang, C. Zhang, Y. Lin, J. Lv, S. Hu, S. Zhang and M. Li, *Mikrochim. Acta*, 2021, **188**, 56.
160 L. Feng and Y. Zhao, *View*, 2020, **1**, e15.
161 J. Chen, F. Xue, W. Du, H. Yu, Z. Yang, Q. Du and H. Chen, *Nano Lett.*, 2022, **22**, 6156–6165.
162 L. Zhu, K. Yuan, J. Yang, C. Hang, H. Ma, X. Ji, A. Devi, H. Lu and D. Zhang, *Microsyst. Nanoeng.*, 2020, **6**, 30.
163 T. Hang, J. Wu, S. Xiao, B. Li, H. Li, C. Yang, C. Yang, N. Hu, Y. Xu, Y. Zhang and X. Xie, *Microsyst. Nanoeng.*, 2020, **6**, 41.
164 M. Salimi and S. Hosseini, *Sens. Actuators, B*, 2021, **344**, 130127.
165 X. Li, C. Luo, Q. Fu, C. Zhou, M. Ruelas, Y. Wang, J. He, Y. Wang, Y. Zhang and J. Zhou, *Adv. Mater.*, 2020, **32**, 2000060.
166 X. Pan, Y. Qi, Z. Du, J. He, S. Yao, W. Lu, K. Ding and M. Zhou, *J. Nanobiotechnol.*, 2021, **19**, 392.
167 H. Di, Z. Mi, Y. Sun, X. Liu, X. Liu, A. Li, Y. Jiang, H. Gao, P. Rong and D. Liu, *Theranostics*, 2020, **10**, 9303–9314.
168 S. Zhou, T. Hu, G. Han, Y. Wu, X. Hua, J. Su, W. Jin, Y. Mou, X. Mou, Q. Li and S. Liu, *Small*, 2020, **10**, e2004492.
169 L. Ding, L. Liu, L. He, C. Y. Effah, R. Yang, D. Ouyang, N. Jian, X. Liu, Y. Wu and L. Qu, *Anal. Chem.*, 2021, **93**, 15200–15208.
170 C. Wu, J. Dai, X. Li, L. Gao, J. Wang, J. Liu, J. Zheng, X. Zhan, J. Chen, X. Cheng, M. Yang and J. Tang, *Nat. Nanotechnol.*, 2021, **16**, 288–295.
171 H. Zhang, Z. Li, C. Gao, X. Fan, Y. Pang, T. Li, Z. Wu, H. Xie and Q. He, *Sci. Robot.*, 2021, **6**, 9519.
172 X. Shi, Y. Zhang, Y. Tian, S. Xu, E. Ren, S. Bai, X. Chen, C. Chu, Z. Xu and G. Liu, *Small Methods*, 2021, **5**, 2000416.
173 X. Yi, W. Zeng, C. Wang, Y. Chen, L. Zheng, X. Zhu, Y. Ke, X. He, Y. Kuang and Q. Huang, *Nano Res.*, 2022, **15**, 1205–1212.
174 J. Ma, J. Ren, Y. Jia, Z. Wu, L. Chen, N. O. Haugen, H. Huang and Y. Liu, *Nano Energy*, 2019, **62**, 376–383.
175 F. Shi, M. Ding, H. Tong, Y. Yang, J. Zhang, L. Wang, H. Li and Y. Huo, *J. Environ. Chem. Eng.*, 2022, **10**, 107385.
176 X. Xu, R. Zhang, X. Yang, Y. Lu, Z. Yang, M. Peng, Z. Ma, J. Jiao and L. Li, *Adv. Healthcare Mater.*, 2021, **10**, 2100518.
177 J. Shen, M. Ma, M. Shafiq, H. Yu, Z. Lan and H. Chen, *Angew. Chem., Int. Ed.*, 2022, **61**, e202113703.
178 Q. Cai, D. Yang, L. Zhong and P. Yang, *Chem. Mater.*, 2020, **32**, 7492–7506.
179 C. Mao, Y. Xiang, X. Liu, Z. Cui, X. Yang, K. Yeung, H. Pan, X. Wang, P. Chu and S. Wu, *ACS Nano*, 2017, **11**, 9010–9021.
180 Y. Liang, M. Wang, Z. Zhang, G. Ren, Y. Liu, S. Wu and J. Shen, *Chem. Eng. J.*, 2019, **378**, 122043.
181 X. Qu, M. Wang, Mi. Wang, H. Tang, S. Zhang, H. Yang, W. Yuan, Y. Wang, J. Yang and B. Yue, *Adv. Mater.*, 2022, **34**, 2200096.
182 J. Zhang, Y. Lin, Z. Lin, Q. Wei, J. Qian, R. Ruan, X. Jiang, L. Hou, J. Song, J. Ding and H. Yang, *Adv. Sci.*, 2022, **9**, 2103444.